UNIVERSITÀ DEGLI STUDI DELLA TUSCIA DI VITERBO

DIPARTIMENTO DI SCIENZE E TECNOLOGIE PER L'AGRICOLTURA, LE FORESTE, LA NATURA E L'ENERGIA (DAFNE)

CORSO DI DOTTORATO DI RICERCA

Biotecnologie Vegetali - XXIV Ciclo

Metabolic changes and physiological responses induced by space ionizing radiation in *Chlamydomonas reinhardtii* D1 mutants

BIO/11

Coordinatore: Prof. Stefania Masci

Firma .....

Tutor: Dott. Giuseppina Rea

Firma .....

Dottorando: Dott. Sandro Pastorelli

Firma .....

To the people those have been closer to me:
my family that support me during this path…

1 - INTRODUCTION

1.1 Cosmic Radiation

The space environment is permeated by fluxes of complex radiation having variable energy and intensity. The Earth atmosphere is able to filter space radiation protecting living organisms from their deleterious effects deriving mainly from ionisation events.

According to its origin space radiation is classified as:

i) Galactic Cosmic Radiation, (GCR) composed by 87% protons, 12% alpha particles and 1% High Z Energetic particle - HZE with energies ranging from 1 and 10^3 GeV deriving by acceleration of stellar flares, supernova explosions, pulsar spin-offs, or from the explosions of nascent galactic nuclei within our galaxy. ii) Solar Particle Radiation, (SPE) consisting of charged particles in large clouds, mainly protons with an energy of about 1GeV. Solar radiation has lower energy compared to galactic cosmic radiation, but its production may be intense and is generally unpredicTable although it appears to reach a peak about every 11 years. There is a significant anti-correlation between solar activity and the intensity of the cosmic rays with energy values under approx. 10 GeV (O'Brien and Sauer, 2003). During the quiet sun period, no energetic particles in the solar wind can reach the sea level on Earth, because of the low energies of the particles. In the active sun period, the solar wind increases by factors of the order of 10^6, making it far denser than the galactic particle flux.

However, there is a more important aspect of the solar cycle than the increased particle flux. The active sun with its large solar wind creates a large distortion of the magnetic field about the Earth (the magnetosphere), which increases the Earth's shielding against intragalactic cosmic rays. This phenomenon leads to a net reduction of the sea-level cosmic rays during the period of the active sun.

iii) Geomagnetically Trapped Particle (GTP) radiation, generated by the interaction of space radiation with the Earth's geomagnetic field, comprising electrons with energies up to 7 MeV, protons with energies up to 600 MeV, and low energy heavy ions. Some of the particles from the Sun get trapped and collected by the Earth's magnetic field (Bert CW and Hyler,1962).

1.1.1 Cosmic rays in the Earth atmosphere

When space ionizing radiations particles collide with other atmospheric particles in our troposphere (*e.g.*: water molecules) disintegrates into smaller pions, muons and other particles forming the so called cosmic ray shower.

Except for protons and electrons near the top of the atmosphere, all particles are produced by interactions of the primary cosmic rays with the air. Muons and neutrinos are produced by decay of charged mesons, while electrons and photons originate by decays of neutral mesons.

The cosmic radiation incident at the top of the terrestrial atmosphere includes all sTable charged particles and nuclei with lifetimes of order 10^6 years or longer. Technically, "primary" cosmic rays are those particles accelerated at astrophysical sources and "secondary" are those particles produced in interaction of the primaries with interstellar gas. Thus electrons, protons and helium, as well as carbon, oxygen, iron, and other nuclei synthesized in stars, are primaries. Nuclei such as lithium, beryllium, and boron (which are not abundant end-products of stellar nucleosynthesis) are secondary. Antiprotons and positrons are partly, if not entirely, secondary, but the fraction of these particles that may be primary is a question of current interest (Miroshnichenko, 2003).

The incoming charged particles are modulated by the solar wind, the expanding magnetized plasma generated by the Sun, which decelerates and partially excludes the lower energy galactic cosmic rays from the inner solar system. In addition, lower-energy cosmic rays are deflected by the Earth's magnetic field although the protection is greater in the equatorial regions than at the poles. There is also some protection by the solar inter-planetary magnetic field and by the stratospheric absorption of low energy particles (Heinrich et al., 1999).

The Earth is well shielded by its atmosphere, but the dose may be significant in prolonged high altitude or space flight. Measurements of this type of radiation have been taken from high altitude aircraft. Fortunately the annual dose is relatively low in constantly exposed air crew (O'Brien et al., 1998).

The incident particles, protons and neutrons, interact with atmospheric matter primarily with the strong interaction. The particles which are considered active in a cosmic ray cascade are reviewed in Table 1.

Particle	Interaction type			Mass (MeV)	Lifetime
	Electromagnetic	Strong	Weak		
Pions	•	•		~134	~26 ns
Muons	•		•	~106	~2 µs
Neutrons		•		940	12 min
Protons	•	•		938	STable
Electrons	•			0.5	STable
Photons	•				STable

Table 1. Active particles in a cosmic ray cascade.

1.1.2 Cosmic influence on chemistry of Earth atmosphere

As we know the solar cycle drives solar irradiance variability in the UV region and also regulates the energetic particle fluxes, which are important for atmospheric chemistry and ozone (Crutzen et al., 1975; Heath et al., 1977; Fabian et al., 1979). While most of the atmospheric particle effects are in the thermosphere and mesosphere, some particle effects occur in the stratosphere and troposphere. The stratospheric odd nitrogen (NO_y, where NO_y = $N + NO + NO_2 + NO_3 + 2*N_2O_5 + HNO_3 + HNO_4 + ClONO_2 + BrONO_2$) content is influenced directly by GCR, which produces NO, in the lower stratosphere, and by solar proton events SPEs, which produce NOy in the upper stratosphere. Both SPEs and precipitating electrons produce NOy in the mesosphere and lower thermosphere, which could be transported downwards and possibly affect the upper stratospheric NOy balance. Jackman (Jackman et al., 1991; 1993; 2000) has reviewed the state of knowledge of the effects of charged particles on NOy and ozone in the middle atmosphere.

Rapid chemistry is initiated after N_2 dissociation and most of the atomic nitrogen is rapidly converted to NO and NO_2**.** The precipitating particle-produced NO constituents can then deplete ozone through the well-known catalytic reaction cycle:

$$NO + O_3 \text{ --> } NO_2 + O_2$$
$$NO_2 + O \text{ --> } NO + O_2$$

A rich array of literature exists on the theory of charged particle production of HOx, which reacts with odd oxygen to cause a loss in ozone (Solomon et al., 1981) by a similar catalytic cycle:

$$OH + O \rightarrow H + O_2$$
$$H + O_3 \rightarrow OH + O_2$$
$$\text{Net: } O + O_3 \rightarrow 2O_2$$

It should be noticed that ozone change at 50 km and at higher altitudes regulates the ozone content practically at all altitudes due to its influence on the solar radiation flux penetration. Ozone observations, which occur during SPEs, support the idea of ozone destruction by solar protons (Krivolutsky et al., 2002).

Earth climate has been varying during all geologic time evolution. The origin of these variations has previously, and almost exclusively, been attributed to internal causes. For

example volcanic dust in the stratosphere can cause cooling of the order 0.5°C for a year or more. The same is assumed for the atmospheric/ocean oscillation in the Pacific called El Niño Southern Oscillation. It is expected that the annual variations in temperature will be a composite of several causes, of which only one is a solar influence. However, at time scales greater than 10 years it looks like the Sun has a significant influence on climate variations. This statement is based on the qualitative agreement between isotopes data about the Earth's temperature over the last 1000 years. A remarkable correlation between cosmic ray flux and variations in the Earth's cloud cover has been demonstrated (Svensmark, 2000).

1.1.3 Effect of Radiation interactions with matter

1.1.3.1 Chemistry

Living and not living matter can be affected by radiation coming from space. Interaction mechanisms are different depending on the type and the energy of the radiation as well as the characteristics of the penetrated matter.

Samples exposures with charged particles having high kinetic energies, result in ionization and excitation of the component, causing an electron loss from a molecule of a certain material. This interaction depends on the atomic make-up of the material and much less on the molecular structure. Also high energy photons of X- and gamma-rays knock electrons off atoms or molecules.

The particles able to ionize molecules are called ionizing radiation. Some examples are:

- Heavy charged particles such as protons, alpha particles, energetic nuclei, mesons;
- Light charged particles such as electrons and positrons;
- Electromagnetic radiation such as X-rays and gamma rays;
- High energy neutral particles such as neutrons;

The unique interaction characteristics of different particles and radiations will affect the severity of physiological damage during exposure of living systems to radiation.

Modes of interaction. There are five basic ways in which radiation interacts with matter: ionization, kinetic energy transfer, molecular and atomic excitation, nuclear reactions, and radiative processes.

• **Ionization** is the removal of an atomic electron from an absorber atom to form an ion pair consisting of a negative electron and a more massive positive ion. Primary ionization is initiated directly by the incident radiation. Secondary ionization is produced subsequently by

the ions created in the primary ionization event. The amount of energy needed to form an ion pair varies with the type of absorbing medium.

- **Kinetic energy transfers** are interactions that impart kinetic energy to ion pairs above the amount required to form the pair. Kinetic energy transfers may also occur due to elastic collisions between the incoming radiation and the nuclei of the absorber.
- **Molecular excitation and atomic electron excitation** are modes of interaction that may occur even when the energy transferred is less than the absorber ionization energy. As the atomic electrons fall back to lower energy levels, x rays and Auger electrons will be emitted. Molecular excitation occurs through translational, rotational, and vibrational processes, and also through electronic excitation. The molecular excitation energy is eventually dissipated by bond rupture, luminescence, or evolution of heat.
- **Nuclear reactions** of incoming radiations with nuclei of absorber atoms can be important modes of interaction. This is especially true for high-energy charged particles and neutrons.
- **Radiative processes** are those in which electromagnetic energy is released by decelerating high-velocity particles.

Radiations can be divided into two groups: charged and uncharged. Charged particles include both unsTable atomic nucleus (α and β particles) and light varieties (photon). Uncharged radiations include γ-rays, x rays, neutrinos, and neutrons. These two groups of radiations have characteristic differences in their interactions with matter. Charged radiation interacts primarily with the electrons of the atoms in the absorbing medium through a series of many small energy-loss events. These events will result in the formation of ion pairs, kinetic energy transfers, and atomic or molecular excitation. Therefore, these radiations lose energy in an incremental and rather predicTable manner.

Uncharged radiations, in contrast, interact less frequently, or not at all, with the absorber electrons while dissipating their energy. Instead of a series of small sequential interactions, the uncharged radiations often undergo one or only a few major interaction events in which all their energy is lost. These interactions are not so predicTable as those for charged particles. It is possible for uncharged radiations to pass through a large amount of matter with a low probability of interaction. This is not the case for charged particles. Hence, uncharged radiations are much more penetrating than charged particles of the same energy (Turner, 1995).

Heavy Charged-Particle Interactions. Heavy charged particles may be considered to include those with masses greater than one dalton. In radioactive decay processes, these

particles have a positive charge. The heavy charged particles interact with matter primarily through ionization. For high-energy particles, nuclear reactions may also be important. The heavy charged particles are much more massive than the electrons with which they are interacting. Therefore, they are not significantly deflected by these interactions and the path of the particle through an absorber is relatively straight. Rarely, however, elastic collisions with the absorber nuclei will result in significant deviations of individual particles from a straight path (Rutherford scattering).

Alpha particles are the most commonly encountered heavy charged particles in radiochemistry. The high likelihood of interaction of positively charged particles with absorber electrons combined with their straight interaction path suggest that the particles will have a fairly well-defined range in a given absorber. The range of the particle may be stated in a variety of units, all of which reflect the distance travelled through the absorber until the particle is "stopped" (i.e., reaches the ambient average kinetic energy of the absorber atoms).

The main reasons that gamma rays and neutrons are interesting in interaction radiation-matter are described below:

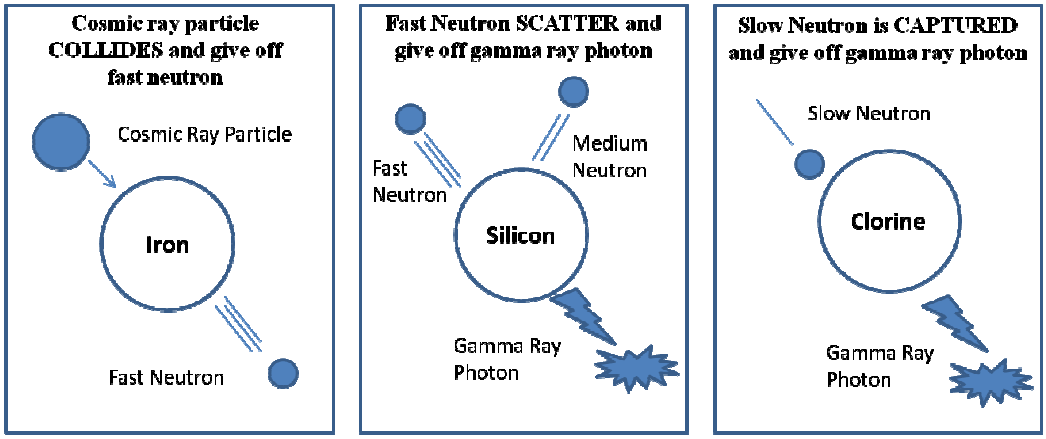

Figure 1 Examples of radiation interactions with matter.

In the first drawing of Figure 1 a cosmic ray particle collides with a target atom and gives off a fast neutron. It is a “collision event.” In the second drawing, a fast neutron bounces off of a target atom and slows down to a medium neutron. It is a “scatter event.” A gamma ray photon of a specific energy is given off. In the final drawing, a slow neutron is captured by and excites a target atom which then gives off a gamma ray photon of a specific energy. It is a “capture event”.

1.1.3.2 Gamma-Ray interactions

Because γ rays are electromagnetic radiation, they have no charge and no rest mass. The interactions of γ rays are, therefore, quite different from those experienced by charged particles. Gamma rays are not subject to Coulomb interactions, and so they do not lose energy continuously as do the charged particles.

Generally, the γ ray will experience only one, or perhaps a few, catastrophic interactions with the electrons or nuclei of atoms in the absorbing material. In these interactions, the γ ray either disappears completely or has its energy significantly altered. Ionization takes place, but most events are induced by secondary electrons and not by the primary γ ray itself. Gamma rays do not have discrete ranges. Instead, the intensity of a beam of γ rays is continuously reduced as it passes through matter in accordance with an exponential absorption law. Two major modes of interaction of gamma rays with matter are: i) the photoelectric effect (PE), when a γ ray interacts with an atom in a process that results in the ejection of an electron from the atom and the complete disappearance of the γ ray; ii) Compton scattering (CS), when the γ ray interacts with an atomic electron losing only part of its energy and it is deflected from its original path.

1.1.3.3 Neutron interactions

Neutron interactions with matter are quite different from those of the charged particles or electromagnetic radiation.

The uncharged neutrons interact almost exclusively with nuclei rather than with the atomic electrons. These nuclear interactions include elastic and inelastic scattering, and direct interactions. The capture of a neutron by a nucleus results in the subsequent emission of a charged particle or γ ray. This is used as the basis for detecting neutrons. Neutron ranges in matter longer than those of the charged particles with comparable or even greater energies.

Thermal neutrons	Most probable energy ~ 0.025 eV Average energy as ~ 0.04 eV
Epithermal neutrons	$0.1 < E_n < 1$ eV
Resonance region neutrons	1 eV < E_n < 1 keV
Fast neutrons	$0.5 < E_n < 2+$ MeV
Neutron generator fast neutrons	14.7 MeV

Table 2. Categories of Neutrons.

The type of interaction that a neutron will experience depends on its energy. Low-energy neutrons (with a mean energy of about 0.04 eV) are called slow or thermal neutrons. They undergo both elastic scattering and direct interactions. The direct interactions experienced by thermal neutrons are most often of the radiative capture type. In this kind of reaction, the neutron is captured by a nucleus, resulting in an excited state that de-excites by emission of a γ ray. As the neutrons increase in energy from thermal to epithermal to resonance to fast, the probability of radioactive neutron capture generally decreases. Energies associated with these different categories of neutrons are given in Table 2.

1.1.3.4 Effect on living cells

When an electron passes through a cell, it releases its energy along its path (called a track) by interacting with the electrons of nearby molecules. The released energy is absorbed by atoms near the track, resulting in either excitation (a shift in the orbit of an electron to a higher energy level) or ionization (release of an electron from the atom). What differs from an ordinary chemical reaction is that when radiation donates energy to atoms or molecules, electrons other than those on the most outer orbit can be released, which makes the atoms very unsTable. Such unsTable atoms are called radicals and are chemically very reactive. Some radicals are so reactive that they exist only for as short a time as a microsecond.

Because the radiation causes ionization and excitation with a random process in the medium, the most abundant molecules have higher probability to undergo with the radiation effect. The biological matrix is composed for 70-90% by water and most of the absorbed energy is caught by water molecules. In order to understand the biological effect of radiation, it is important to describe the radiochemistry of water.

1.1.4 Radiochemistry of water

Bombarding liquid water with high energy photons or charged particles causes excitation and ionization of the water molecules (Figure 2).

The excitation of a molecule of water causes the prompt dissociation to the two radicals $H^{\bullet}$ $OH^{\bullet}$:

$$O\,H_2 \rightsquigarrow H_2O^{*} \longrightarrow H^{\bullet} + OH^{\bullet}$$

The *ionization* can give the water radiolysis producing an electron and a water molecule with a positive charge:

$$H_2O \rightsquigarrow H_2O^{+} + e^{-}$$

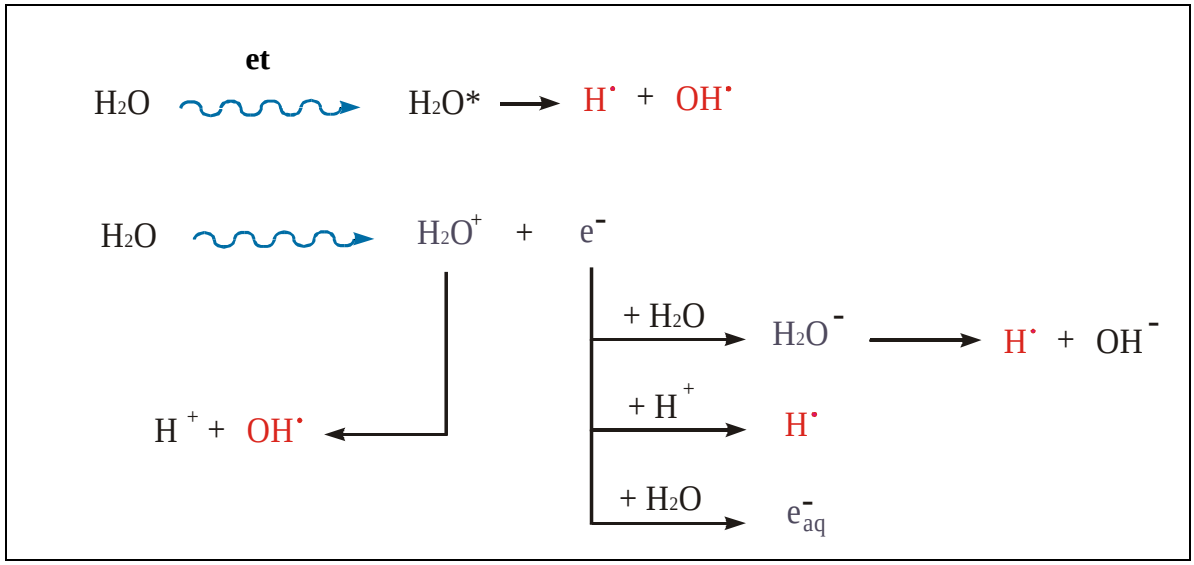

Figure 2. Radiation interaction with molecules of water (Alpen ,1990).

The primary radical species formed in the radiolysis of liquid water are solvated electrons, hydroxyl radicals and hydrogen atoms. H_2O_2, H_2 and H_3O^{+} are also formed.

To some extent, presolvated electrons and H_2O^{+} recombine in the tracks, producing an excited water molecule, which can dissociated again to $HO^{\bullet}$ and $H^{\bullet}$ (Figure3)**.** At very high water concentrations, some electrons can be scavenged in their presolvation state by the solute, resulting in a higher yield of scavenged electrons relative to the values from dilute solution. Yields of products such as $HO^{\bullet}$ and $H^{\bullet}$ are correspondingly reduced.

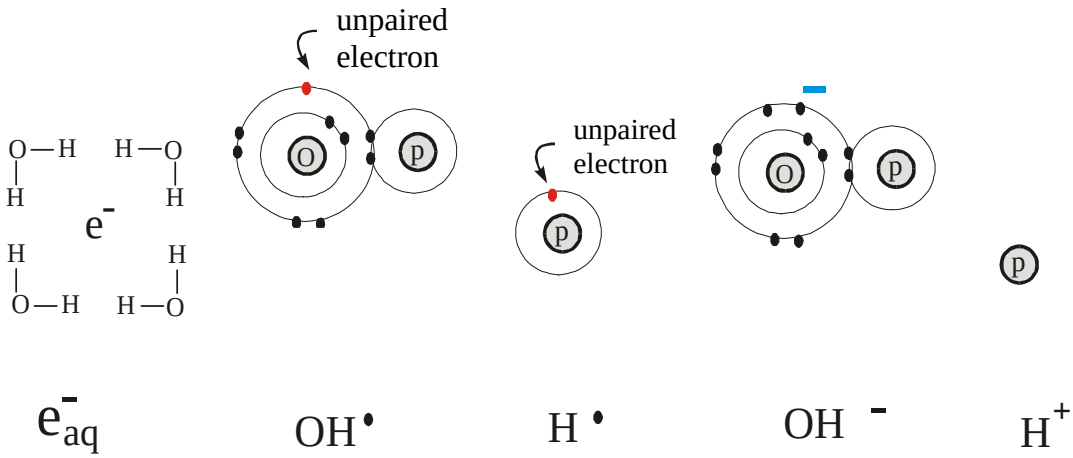

Figure 3. Main products from interaction of the radiation with water molecules.

Inside the organic matter, free radicals produced by water radiolysis, can react with organic, biologically important molecules, causing damages. Moreover, the biological effectiveness of radiation can be enhanced by the oxygen. As matter of fact, if the matter hit by ionizing radiation contains dissolved oxygen, the chemical reactions of free radicals with oxygen produce superoxide, hydroperoxyl radicals and hydrogen peroxide:

- $e^-_{aq} + O_2 \longrightarrow O_2^{\bullet -}$ (anion radical superoxide)
- $H^\bullet + O_2 \longrightarrow H_2O^\bullet$ (hydroperoxyl radical)
- $O_2^{\bullet -} + H^+ \longrightarrow H_2O^\bullet$ (hydroperoxyl radical)
- $H_2O^\bullet \longrightarrow H_2O_2$ (hydrogen peroxide) + O_2

Reactions of superoxide and hydroperoxyl radicals are studied because of their role in biological systems. The products of the reactions have a harmful power higher than primary radicals, because they show a big affinity with the molecules.

1.1.5 Interaction with organic matter

In general, radiation-induced ionization may act directly on the cellular component molecules or indirectly on water molecules, causing water-derived radicals (Figure 4).

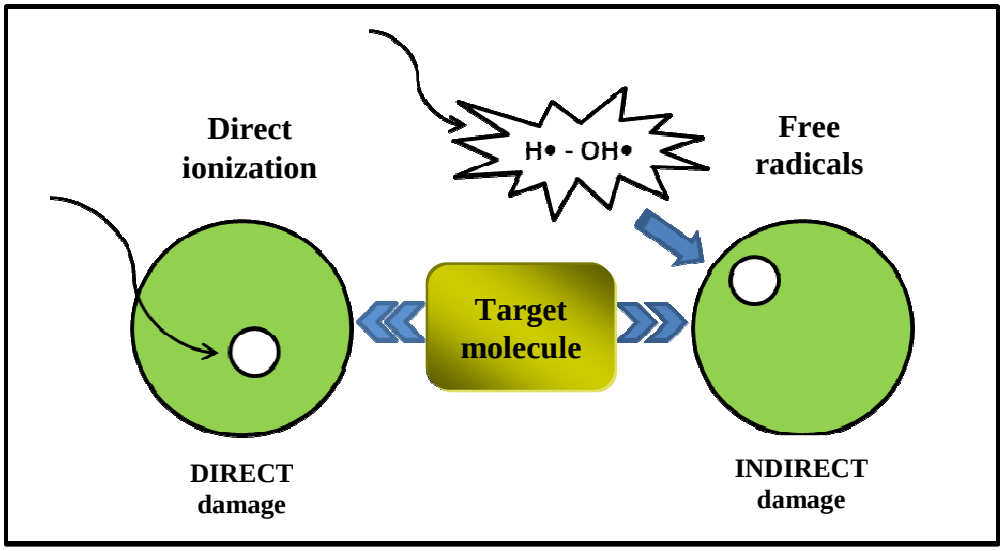

Figure 4. Direct and indirect action of ionizing radiation.

Radicals react with nearby molecules in a very short time, resulting in breakage of chemical bonds or oxidation of the affected molecules. For examples free radicals can extract hydrogen from organic molecules (RH) forming secondary radicals $R^{\bullet}$ (Coggle, 1998):

$$RH + OH^{\bullet} \longrightarrow R^{\bullet} + H_2O$$
$$RH + H^{\bullet} \longrightarrow R^{\bullet} + H_2$$

Secondary radicals, which can again react with other molecules, are formed also for direct action of ionizing radiation:

$$RH \rightsquigarrow R\,H^{+} + e^{-} \longrightarrow R^{\bullet} + H^{+}$$

If a organic molecule is transformed directly or indirectly in a free radical it can react with oxygen in the following way:

$$R^{\bullet} + O_2 \longrightarrow RO_2^{\bullet}$$

A chain reaction can involve several RH:

$$RO_2^{\bullet} + RH \longrightarrow RO_2H + R^{\bullet}$$

Proteins and desossiribonucleic acid (DNA) are organic macromolecules (R) with a fundamental biological role inside living cells.

The major effect in cells is DNA breaks. Since DNA consists of a pair of complementary double strands, breaks of either a single strand or both strands can occur. However, the latter is believed to be much more important biologically. Most single-strand breaks can be repaired normally thanks to the double-stranded nature of the DNA molecule (the two strands complement each other, so that an intact strand can serve as a template for repair of its damaged, opposite strand). In the case of double-strand breaks, however, repair is more difficult and erroneous rejoining of broken ends may occur. These so-called misrepairs result in induction of mutations, chromosome aberrations, or cell death.

It is clear that exposure of biological material to ionising radiation could leads to a loss of function due to the modification of critical structures (Beauregard and Potier, 1985). One of the most important and discussed problems in radiation protection concerns the determination of the biological effectiveness of radiation on living organisms. In order to assess the radiation risk for living beings during long-term spaceflights, it is very important to clarify whether combination of cosmic radiation and other factors have a synergistic effect on the cell functions.

1.1.6 Definitions of used quantities

It is useful to outline some information about parameters utilized to determine Ionizing Radiation effect on living matter. Up to now, the human body is taken as reference (ICRP, Publication 74).

- Linear energy transfer (LET) is a measure of how, as a function of distance, energy is transferred from radiation to the exposed matter. A high value of LET indicates that energy is deposited within a small distance. It is also known as the restricted linear collision stopping power. High LET radiation: Radiation with high linear energy transfer, normally assumed to comprise protons, neutrons and alpha particles (or other particles of similar or greater mass).

Low LET radiation: Radiation with low linear energy transfer, normally assumed to comprise photons (including X rays and gamma radiation), electrons, positrons and muons.

- Absorbed dose (denoted as D) is the quotient of $d\bar{\varepsilon}$ e by d*m*, where de is the mean energy imparted by ionizing radiation to matter of mass d*m*, thus

$$D = \frac{d\bar{\varepsilon}}{dm}$$

The unit of absorbed dose is joule per kilogram ($J \cdot Kg^{-1}$ or *gray: Gy*).

- Dose Equivalent (denoted as H) is the product of Q and D at a point in tissue, where D is the absorbed dose and Q is the quality factor for radiation at that point, thus

$$H = QD$$

The unit of Dose Equivalent is joule per kilogram ($J \cdot Kg^{-1}$ or *sievert: Sv*).

- Ambient Dose Equivalent (denoted as H*(d)), at a point in radiation field, is the dose equivalent that would be produced by the corresponding expanded and aligned field in the ICRU sphere at a depth d, on the radius opposing the direction of the aligned field. The unit of Ambient Dose Equivalent is joule per kilogram ($J \cdot Kg^{-1}$ or *sievert Sv*).
- Equivalent Dose in a Tissue T (denoted as $H_{T,R}$) is the absorbed dose in an organ or tissue multiplied by the relevant radiation weighting factor (see Table 3), thus

$$H_{T,R} = w_R D_{T,R}$$

where $D_{T,R}$ is the absorbed dose averaged over the tissue or organ T, due to radiation R, where w_R is the radiation weighting factor for radiation R.

When the radiation field is composed of radiations with different values of w_R, the absorbed dose is subdivided into blocks, each multiplied by its own value of w_R and summed to determine the total equivalent dose, i.e.

$$H_T = \sum_R w_R D_{T,R}$$

The unit of Equivalent Dose is joule per kilogram ($J \cdot Kg^{-1}$ or *sievert (Sv).*

- Effective Dose Equivalent (denoted as H_E) is the weighted average of the dose equivalents, each weighted by a tissue or organ weighted factor, thus:

$$H_E = \sum_T w_T H_T$$

where H_T is the dose equivalent in tissue T, and w_T is the is the weighting factor for tissue T, as formerly recommended by ICRP.

Types of radiations and energy intervals	**Weighting factors of radiation, wR**
Photons, all energies	1
Electrons, all energies	1
Muons, all energies	1
Neutrons energies:	
< 10 keV	5
10 – 100 keV	10
100 keV – 2 MeV	20
2 – 20 MeV	10
> 20 MeV	5
Protons, (not recoil protons) with energy < 2MeV	5
Alphas, fission fragments, heavy nuclei	20

Table 3. Values for radiation weighting factors (ICR, Publication 60).

Sanitary effects of ionizing radiation. Radiation exposure can determine risks of sanitary effects for living beings and requires adequate radio-protective precautions. Induced effects on men can be distinguished in somatic effects and genetic effects, distinguishing if they reveal their effect on the exposed individual or on his descendent. A lot of somatic effects are non – stochastic effects. Their seriousness is related to dose absorbed by the considered organ or tissue and each non-stochastic effect is characterized by a threshold value of absorbed dose. Only if the absorbed dose is higher than the threshold value, the effect appears. Threshold dose values, for different deterministic effects, are always very high and they are known with a good precision. All genetic effects and the most important somatic effects (as leukaemia, tumour) are stochastic effects. They are characterized by the absence of a threshold dose value and they occur with a probability that depends on the absorbed dose value.

1.1.7 Biological space studies

The main difficulties for the permanence of biological organisms in space (including man) are caused mainly by the presence of ionizing radiation, microgravity, high-temperature and high vacuum conditions. During the time, the enhanced science community interest on space biology was followed by the increased number of space missions aimed to understand space environmental effects on living organisms.

Permanence in space can result in a number of adverse effects such as bone loss, skeletal muscle atrophy, cardiovascular problems, immune system disregulation, alteration of sleep and circadian rhythms, cancer, cataracts and possible damage to the central nervous system which are mainly associated to the occurrence of microgravity and exposures to the GCR environment (Hellweg and Baumstark-Khan, 2007).

Plants are essential companion lifeforms for long-term space missions, where Human habitats must mimic the cycles of life on Earth to generate and recycle food, oxygen, and water. Photosynthetic organisms on the International Space Station (ISS) could be use as life supporting system, supplying oxygen and removing carbon dioxide from the station atmosphere. They also prevent gases like ammonia and acetone, which people emit in small amounts, from building up to dangerous levels.

The majority of biological studies on the physiological effects of space have been concerned with the gravitropic responses of higher plants. Nowadays, numerous are the scientific data available on this topic.

Microgravity is one of the space environmental condition affecting cell division, cell components and their distribution. Many studies focused on the effects of Space radiation and/or microgravity on the number, viability, kinetics of germination, growth rate and mutation frequency of spores formed in Space (Takahashi, 2001). Dormant seeds do not appear to be sensitive to gravity. However, during development, mitosis and cytokinesis, plants appear to be influenced by the absence of gravity. Mitosis is disturbed in the absence of gravity, as demonstrated by reduced or inhibited cell division, anomalies in the separation of chromosomes and the fragmentation of the chromatids (Kordyum, 1997). Not only Space radiation can interfere with biological process, but also space flights appear to alter the process of differentiation particularly in root tissues, perhaps on account of an altered hormonal equilibrium. *Chlorella vulgaris* cells grown during a space flight differred from controls showing a reduction in the amount of polysaccharide reserves in chloroplasts. Increased concentrations of mono and disaccharides resulted in the increased activity of amylases. Rearrangements in chloroplast structure, such as the decrease of polysaccharide

reserves were probably due to an increase in hydrolytic processes by microgravity (Popova and Shniukova, 1995).

The absence of gravity seems to affect also the organelles membranes, as evidenced by the destruction of the grana and the detachment of the thylakoids in the chloroplast stroma in seedlings grown in space (Nedukha, et al., 1999).

Additional consequences include the deformation of the endoplasmic reticulum, the swelling of the mitochondria, aggregation of the chromatin and the presence of multiple nucleoli within the nucleus. These changes suggest a major influence of space condition on the growth and development of micro-organisms (Nedukha, 1997; Kordyum, 1997).

The relationship between gravity and the processes of growth and development of photosynthetic organisms can only be determined by eliminating gravity, as occurs in space.

Space environment affects almost all biological processes, in particular germination and flowering. Embryo lethality and lethal mutation frequency were observed in *Arabidopsis thaliana* seeds (Kranz, 1990) and in other organisms such as *Escherichia coli* and *Bacillus subtilis* (Horneck, 1995).

Despite the numerous study on plant response under microgravity condition, very little is still known about the effects of ionizing radiation on the photosynthetic apparatus (Sakashita, 2002; Saakov, 2003).

A limiting factor in this research field is that there are very appreciable temporal variations in both radiation composition and intensity (Internet site on Solar chart: http://hiraiso.crl.go.jp/). For these reasons, measuring and reproducing ground space radiation in all its components is a nearly impossible task. Up to date, the best approach to study radiation effect is utilizing single beam, produced on ground by properly equipped facilities.

Unicellular organisms were the first subjects in biological studies in Space. Rapid multiplication, tiny size and simple procedure to keep growth conditions are the advantages in using these simplest biological systems to estimate cosmic radiation effect (Nechitailo, 2001).

In on ground studies, several investigations have been focused on microorganisms able to survive to high doses of ionizing radiation like *Micrococcus radiodurans* (Hansen, 1982), *Deinococcus radiodurans* (Venkateswaran, 2000), *Chroococcidiopsis* cells (Billi, 2000) and *Archeon Pyrococcus abyssi* (Jolivet, 2003).

1.2 Photosynthesis and Photosystem II Complex

1.2.1 The oxygenic photosynthesis

Solar radiation is an example of ionizing radiation exploited by photosynthetic organisms for photosynthesis, the physico-chemical process by which plants, algae and certain bacteria convert light energy into chemical energy of organic compounds, with concomitant use of these components in the bioenergetic processes. In plants, algae and cyanobacteria, the photosynthetic processes result in the fixation of carbon dioxide (CO_2) from the atmosphere that is used to synthesize carbohydrates and release of molecular oxygen to the atmosphere. This process is known as oxygenic photosynthesis.

The first step in photosynthesis is the absorption of photon by a pigment molecule of photosynthetic antenna resulting in conversion of the photon energy to an excited electronic state of pigment molecule. The antenna consists of hundreds of pigment molecules (chlorophylls, bacteriochlorophylls, carotenoids, etc.) that are bounded to proteins within the photosynthetic membrane. The excited electronic state is transferred over the antenna molecules as an exciton. Some excitons are converted back into photons and emitted as fluorescence, some converted to heat. For most of the excited pigment molecules the most useful decay pathway is “energy transfer” to a photochemical reaction centers, and it is of vital importance to photosynthesis. Excitons trapped by a reaction center provide the energy for the primary photochemical reaction of photosynthesis – the photoinduced transfer of an electron. Subsequent electron transfer reactions occur in the dark which results in accumulation of chemical bound energy. Electron transfer reactions in photosynthesis involve electron carriers or electron-transfer proteins, among others, (bacterio) chlorophylls, quinones, cytochromes, and iron-sulfur proteins that has been recently reviewed by Feyziyev (2010).
Electron transport chain trough specialized protein, called photosystem two (PSII) and photosystem one (PSI) protein complex, leads to convert light energy into chemical energy and reducing equivalents, adenosine triposphate (ATP) and nicotinamide adenine dinucleotide phosphate (NADPH), which are used in the CO_2 fixation to produce carbohydrates $(CH_2O)n$ (Mitchell, 1961). Oxygenic photosynthesis is driven by visible light (wavelengths from 400 to 700 nm) that is absorbed by different pigment molecules, chlorophyll *a* and *b*, carotenoids and phycobilins. The pigment molecules are bound to polypeptides forming pigment-protein complexes. Two types of antenna complexes, the inner (core) antenna consisting of pigment-proteins that are an integral part of the reaction center complex, and outer (peripheral) antenna complexes are distinguished in oxygenic species. In plants and green algae the light absorbing

pigment molecules are chlorophyll *a*, chlorophyll *b* and carotenoids. The cyanobacteria and red algae have a different outer antenna system. In cyanobacteria and red algae, the phycobiliproteins are assembled into supromolecular aggregates called phycobilisomes, which are attached to the photosynthetic membrane surface and transfer electronic excitation energy (*via* chlorophyll) to the reaction centers to initiate photochemical reactions. Carotenoids and phycobiliproteins serve as accessory pigments, to absorb light energy not absorbed in the spectral region of chlorophyll absorption and transfer this energy to chlorophylls. The efficiency of singlet-singlet energy transfer from certain carotenoids to chlorophyll may be very high ranging from 70% to nearly 100%. Phycobilisomes can funnel the absorbed energy to the reaction center with more than 95% efficiency (Ke, 2001).

1.2.2 Photosystem II and Reaction Center

The multisubunit pigment-protein complex Photosystem II of higher plants, algae and cyanobacteria is located inside the thylakoid membranes (Figure 5).

Since the existence of oxygenic photosynthesis, it catalyses the light-induced transfer of electrons from water to plastoquinone, oxidizing water molecules to oxygen, sustaining an aerobic atmosphere on Earth. During these reactions reduced equivalents are produce resulting in carbon dioxide fixation, creating biomass, food and fuel.

Its unique properties require an elaborate arrangement of integral membrane proteins, specifically bound pigment moieties, extrinsic proteins and inorganic cofactors. PSII uses light energy to drive two chemical reactions - the oxidation of water and the reduction of plastoquinone. The PSII core is the minimal unit which is capable of catalysing full PSII function. It is composed of a reaction center, which consists of the D1 and D2 polypeptides (encoded by the chloroplast *psbA* and *psbD* genes, respectively), cytochrome b559 (Cyt $_{b559}$), the psbI protein and six chlorophyll (Chl) and two pheophytin (Pheo) molecules, an inner antenna of chlorophyll-binding proteins termed CP47 and CP43, and the extrinsic lumenally bound proteins of the OEC, 33 kDa protein (psbO), 23 kDa (psbP) and 17 kDa (psbQ), in higher plants and green algae, whereas in cyanobacteria psbP and psbQ are replaced by the 15 kDa psbV (cytochrome c550) and the 12 kDa psbU. These intrinsic and extrinsic proteins, together with a number of low-molecular weight subunits make up the core complex (Debus, 1992).

Light is funnelled from the light harvesting complexes to the photochemically active reaction center (RC) of PSII. The RC contains a special form of Chl *a*, P680 (the primary electron donor of PSII), which acts as an exciton trap and is converted to a strong reducing

agent after excitation (P680*), P680* is then photooxidized and donates an electron to the primary acceptor of PSII, a protein-bound pheophytin.

$$P_{680}^{\bullet} \rightarrow P_{680}{}^{+}Phe^{-} \rightarrow {}^{3}Chl^{\bullet}$$

This charge separation is stabilized by the transfer of an electron to a plastoquinone molecule (Q_A), and subsequently to a second plastoquinone (Q_B). On the lumenal side, the oxidized form of P680 is reduced by a redox active tyrosine residue of the D1 protein, TyrZ. The oxidized tyrosine radical TyrZ extracts an electron and a proton from a cluster of four manganese atoms that binds substrate water (Lydakis-Simantiris et al., 1997). The Q_A plastoquinone is a one-electron acceptor, firmly bound to the D2 protein. In contrast, the Q_B plastoquinone is a two-electron acceptor, bound to the D1 protein.

A second photochemical turnover leads to the accumulation of two reducing equivalents on Q_B, which is then released from PSII, as plastoquinol, to be subsequently oxidized by PSI via the cytochrome b_6f complex.

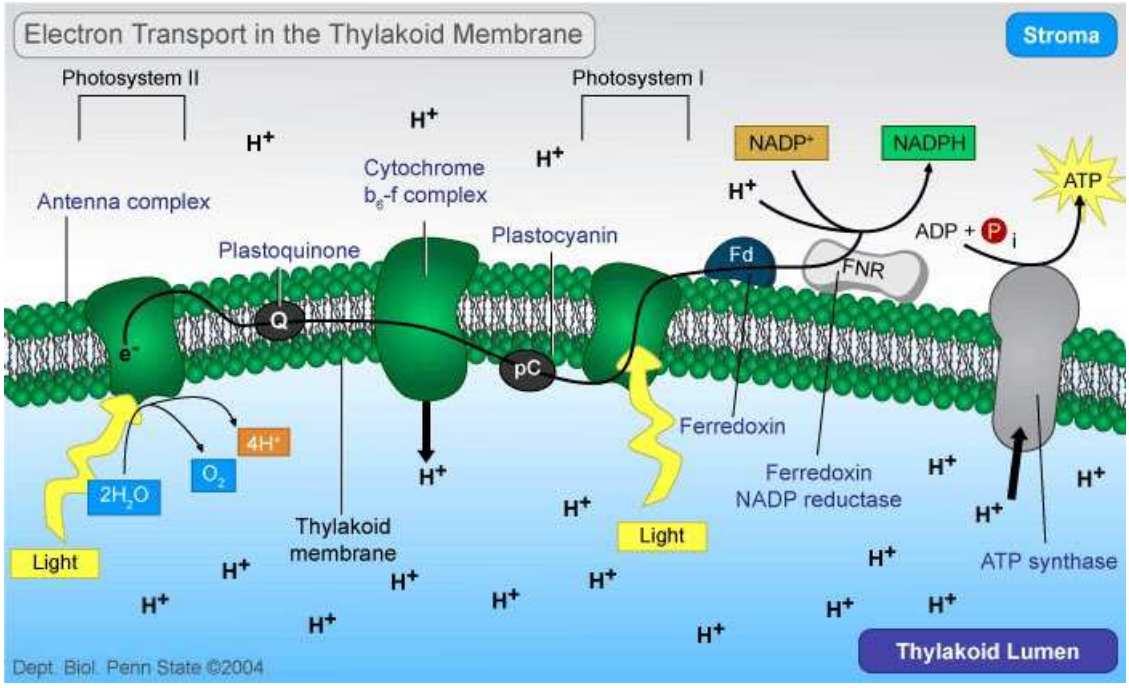

Figure 5. The electron transport pathway of oxygenic photosynthetic organisms.

The empty Q_B site is then occupied by another plastoquinone molecule. Two further photochemical turnovers provide the oxygen-evolving complex with four oxidizing equivalents.

The accumulation of four oxidizing equivalents, in a manner consistent with the observed S-state transitions, leads to the release of molecular oxygen from the complex. During the accumulation of oxidizing equivalents, protons are released to the lumenal space of the thylakoid membrane (Mattoo et al., 1989).

1.2.3 Light absorption - the antenna system

The light-harvesting (or antenna) complex of plants is a protein-pigments complex embedded in the thylakoid membrane. It is formed predominantly by chlorophyll *b*, xanthophylls and carotenoids that transfer light energy to the central chlorophyll *a*, known as core pigment. In order to broad the range of light adsorption each antenna component has a different spectra ranging from 400 to 700 nm. The entirely light harvest complex is constitued by six different type of apoproteins, Lhcb 1‑6.

The native form of LHCII (Figure 6), accounting for about 60% of the total chlorophyll content of thylakoid membranes, is a trimer composed of three Lhcb proteins: Lhcb1, Lhcb2 and Lhcb3 (Lucinski and Jackowski, 2006). Lhcb4, Lhcb5 and Lhcb6 consitute, in turn, the polypeptide moiety of minor peripheral light-harvesting complexes, namely CP29, CP26 and CP24, respectively.

Lhcb1 is constituted by three tylakoid transmembrane α –helices, and also two short lumen-exposed amphipatic α-helices. This protein has the N-terminus of the molecule facing the stroma and the C-terminus penetrating the lumen. Each Lhcb1 binds eight Chl *a* , six Chl *b* and xanthophylls: one neoxanthin, one violaxanthin. The amino acid composition of Lhcb1 is 94 % identical to that of Lhcb2 (Standfuss et al., 2005). Lhcb2 occurs in vivo as a heterotrimer with Lhcb1 while the Lhcb3 constitutes the smallest fraction of LHCII proteins, not exceeding 11 % of the total apoprotein content of LHCII, and differs from Lhcb1 and Lhcb2 in its structure (Lucin´ski and Jackowski, 2006).

Each antenna system has between 250 and 400 pigment molecules and the adsorbed energy is transferred in a resonance way towards the reaction center of each photosystem, where complex chemical reactions capture light energy in the form of chemical bonds.

Under changing light conditions, the antenna complex is fundamental in balancing the excitation energy between photosystems I and II, by the reversible phophorylation of light harvesting chlorophyll *a*/*b* binding proteins (LHCII), helping in the avoidance of possible photo-oxydative damages when hight light condition occur (Kargul and Barber, 2008).

Carotenoids not only actively participate at the harvesting of light energy but they also play a crucial role in prevent the photo-oxidative damages of chlorophyll molecules (Cogdell 2006; van Oort et al., 2007; Barros et al., 2009).

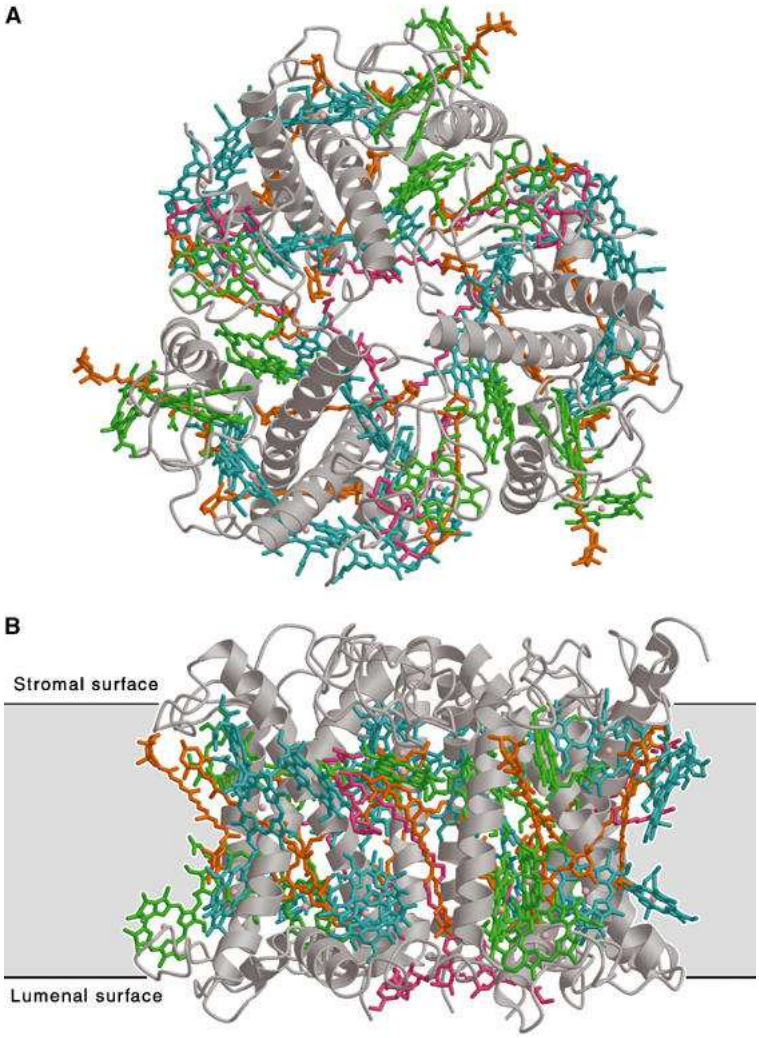

Figure 6. The LHC-II trimer: (**A**) top view from stromal side; (**B**) side view. LHC-II protrudes from a 35A° lipid bilayer (black lines) by 13A° on the stromal side and by 8A° on the lumenal side. Grey, polypeptide; cyan, Chl *a*; green, Chl *b*; orange, carotenoids; pink, lipids (from Standfuss J et al., 2005).

1.2.4 The photosynthetic reaction center D1 protein

D1 is a 32 kDa protein encoded by the plastid *psbA* gene and translated on thylakoid membrane-bound ribosomes. Mature D1 has five transmembrane domains (TMs) with the N-terminus on the stromal side of the thylakoid membrane. Light has an important role in regulation of various stages of D1 synthesis from translation initiation to elongation, maturation and insertion into the thylakoids (Zhang and Aro, 2002).

D1 turnover is also a physiological highly regulated process in photosynthetic organisms: the degradation and synthesis of new D1 protein is genetically regulated and is a stress recovery mechanism (Mulo et al., 2012).

The detection of amino acid mutations specifically in the D1 reaction center subunit is greatly supporting the understanding of PSII structure and function. These discoveries identified the D1 subunit as the "herbicide binding protein". Since the inhibitors tested were known to compete with the native plastoquinone Q_B for its binding site this protein was likely to be also the Q_B binding protein. Furthermore, a specific region within D1 emerged which we now address as herbicide binding. Abundant biochemical and genetic evidence has accumulated which places the binding niche between amino acids 211 and 275.

A number of mutations in the gene *psbA* have been found to confer herbicide-resistance. In algae mutants, mutations at positions 219, 251, 252, 255, 256, 264 and 275 are most common and result in resistance to several classes of herbicides (Oetteier, 1999). All these *psbA* mutations are located on helices IV and V helices and their connecting loop in D1 protein, which is a specific region of the polypeptide between amino acid residues 211 and 275 (Ohad, 1992).

1.2.5 Carotenoids

In oxygenic photosynthetic organisms, carotenoids are the most widespread natural pigments and fulfil a variety of functions. Carotenoids are polyisoprenoid compounds containing 40 carbon atoms. They possess a long chain of conjugated double bonds in the central part of the molecule, and variable end groups: different level of hydrogenation and introduction of oxygen-containing functional groups create a large family of over 600 natural compounds (Green and Durnford, 1996). In higher plants, two different classes are found into thylakoids: (i) carotenes (*e.g.* β-carotene), which are hydrocarbones with linear structure and with cyclic groups in one or both extremities, and (ii) xanthophylls (*e.g.* lutein, zeaxanthin), which are oxygenated derivatives of the first group. In higher plants, the carotenoids normally

associated with thylakoid membranes are α- and β- carotene (bound especially to the core complex of both photosystems) (Green and Durnford, 1996) and the xanthophylls lutein, zeaxanthin, violaxanthin and neoxanthin (bound to antenna complexes) (Formaggio et al., 2001; Caffarri et al., 2001). Carotenoids are non-covalently bound to the protein complexes, probably involving hydrophobic interactions (Gastaldelli et al., 2003).

Carotenoids have three main functions in photosynthesis: a) structure stabilisation and assembly of protein complexes in the thylakoid membrane; b) light absorption and excited state energy transfer to the chlorophylls (Green and Durnford, 1996); c) protection against photo-oxidative damages (Havaux and Niyogi, 1999).

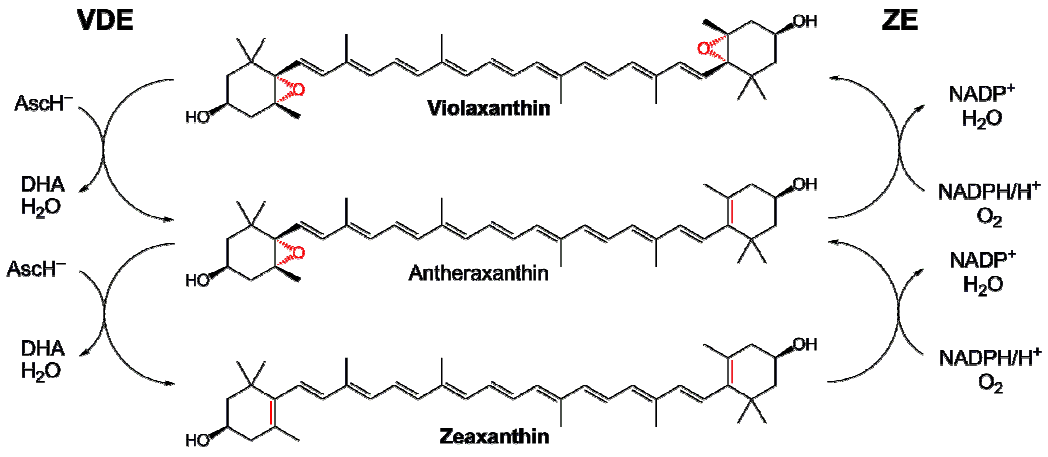

Figure 7. Biosynthetic pathway of β-carotene-derived xanthophylls in higher plants. The arrows between pigments denote enzymatic conversion caused by xanthophyll cycling. Enzymes involved are also reported. Carotenoids involved in the xanthophylls cycle are localized in the peripheral antenna proteins of PSII (Ruban et al., 1999), not in the core complex and inner antenna of PSII. Upon de-epoxidation, the newly synthesized zeaxanthin is distributed among LHCII and minor antennae.

Carotenoids composition of thylakoid is not constant: it can undergo modifications during long-term acclimation of plants to stressing condition, as well as rapidly changes following fluctuations of solar light intensity (Green and Durnford, 1996). The xanthophylls cycle (Figure 7) involves the three xanthophylls violaxanthin, antheraxanthin and zeaxanthin, and consists in a light-dependent, reversible de-epoxidation of violaxanthin to zeaxanthin *via* the intermediate antheraxanthin; the former reaction is catalysed by violaxanthin deepoxidase (VDE), a lumenal enzyme activated by acidification of the luminal compartment (Green and Durnford, 1996).

1.2.6 Carotenoids and plastoquinone biosynthesis

In vascular plants and algae carotenoids are usually synthesized in plastid, which is also the site of their are located. The majority of carotenoids are bound to membrane proteins associated with the photosynthetic apparatus, and to some extent with plastid envelope membranes (Derguini et al., 1991). Green algae are photosynthetic organisms able to accumulate extraplastidic carotenoids under unfavourable conditions. For example, astaxanthin of the green alga *Haematococcus pluvialis* is located in cytoplasmic lipid globules (Boussiba, 2000). The prominent carotenoids in green algae and vascular plants are *β*-carotene, lutein, 9-*cis*neoxanthin, and violaxanthin (Figure 8), being rapidly converted to antheraxanthin and zeaxanthin under high light conditions, as reported above. The carotenogenic enzymes are encoded by nuclear genes in *Chlamydomonas reinhardtii*. Biosynthesis of carotenoids (Figure 8) is initiated with the formation of isopentenyl-diphosphate (IPP), called "active isoprene." The subsequent reaction sequences are often divided into four stages: (*a*) stepwise condensation of isoprene units to form the first carotenoid, phytoene, (*b*) extension of the π-electron system by sequential desaturation resulting in lycopene formation, (*c*) cyclization reactions that generate the carotenes, and (*d*) synthesis of xanthophylls by the introduction of the oxygen functions (Grossman et al., 2004). Sequential addition of three molecules of IPP, results in the formation of the C20-compound geranylgeranyl pyrophosphate (GGPP) (Figure 8). This chain elongation is catalyzed by the enzyme GGPP synthase. GGPP is not only an intermediate in carotenogenesis, but also a substrate for the formation of a variety of other cellular components, including the phytol moiety necessary for the synthesis of Chl, tocopherols and phylloquinone and, in the case of vascular plants but not algae or bacteria, the hormone gibberellin. In chloroplasts and mitochondria, polyprenyl transferases synthesize the long chain isoprenoid component of plastoquinone and ubiquinone, respectively, by adding isoprene units to GGPP (Figure 8).

Head-to-head condensation of two molecules of GGPP by phytoene synthase (PSY) results in formation of phytoene, the first carotenoid of the pathway. This reaction and all subsequent steps are linked to plastid membranes as the carotenoid substrates are hydrophobic and membrane associated (Schledz et al., 1996; Bonk et al., 1997). As PSY catalyzes the first committed step of carotenoid biosynthesis, it was expected to represent a key target for regulatory control. Experimental evidence supports this expectation. Over-expression of the *psy* gene in tomato plants resulted in dwarf plants because elevated phytoene production in this strain caused a severe reduction in gibberellin synthesis (Fray et al., 1995). Similarly, the

carotenoid content of tomato fruits increased substantially in concert with the fruit-specific expression of a bacterial *psy* gene (Fraser et al., 2002). In vascular plants, *psy* mRNA increases in red light in a phytochrome-dependent manner (Von Lintig et al., 1997). In *H. pluvialis*, expression of *psy* appears to be under photosynthetic redox control because increased transcript accumulation in high light could be prevented by the addition of the herbicide 3-(3,4-dichlorophenyl)-1,1-dimethylurea, which blocks electron transport at PSII (Steinbrenner and Linden, 2001). In *C. reinhardtii*, *psy* mRNA increases following exposure of cells to blue light, suggesting that the gene may be under the control of a blue light photoreceptor such as PHOT1 or CRY1 (Bohne and Linden, 2002).

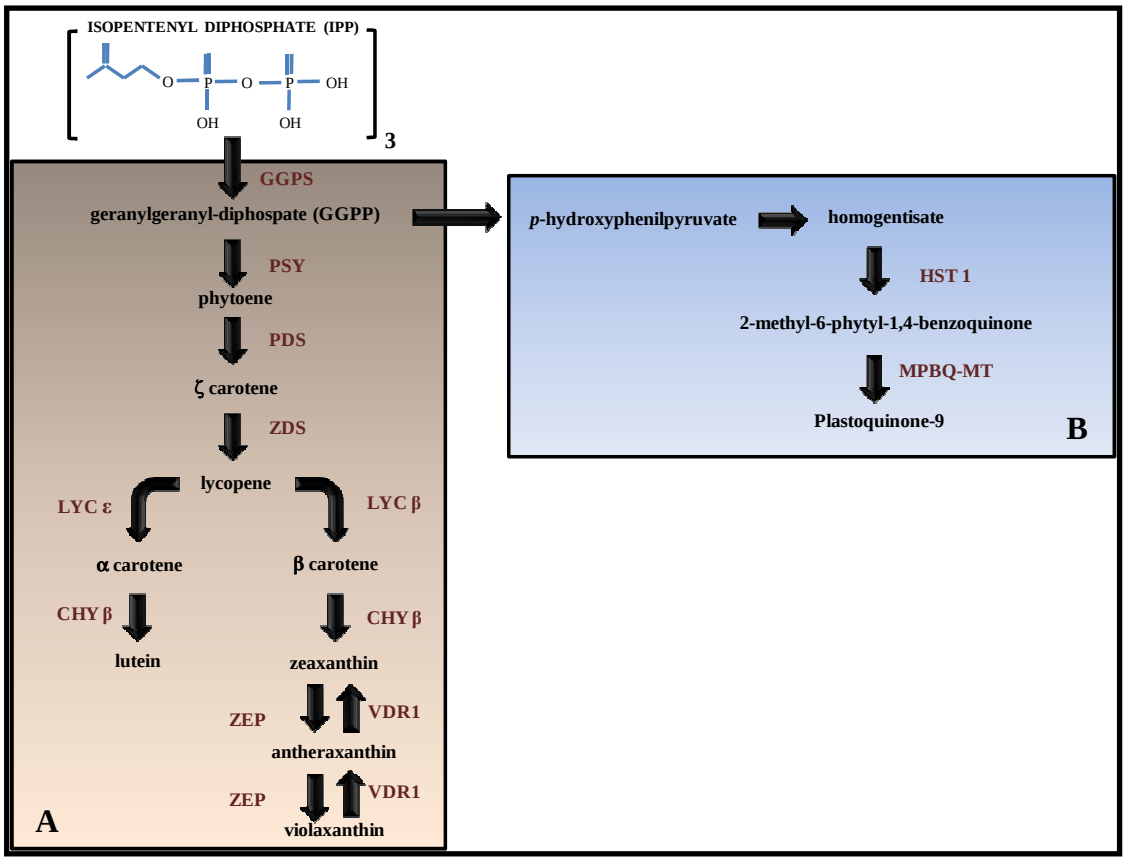

Figure 8. Schematic representation of carotenoids (A) and plastoquinone (B) biosytetic pathways in *C. reinhardtii*

Principal enzymes involved in carotenoids biosynthesis are reported in Figure 8. Phytoene contains only three conjugated double bonds and consequently shows no visible absorbance.

In vascular plants and green algae, two desaturases sequentially introduce additional conjugated double bonds into phytoene, thereby extending the π-electron system and shifting the absorbance to longer wavelengths. These enzymes are structurally and functionally related

and likely have evolved from a common ancestor by gene duplication (Sandmann, 2002). The initial desaturation by phytoene desaturase (PDS) introduces two double bonds into the molecule, resulting in the formation of ζ -carotene. Two additional desaturation steps catalyzed by ζ -carotene desaturase (ZDS) yield lycopene. Both PDS and ZDS contain an amino-terminal conserved dinucleotide binding motif and use FAD as a redox cofactor.

Electrons generated by the reaction are transferred from $FADH_2$ to plastoquinone, and from there can be funnelled either into the photosynthetic electron transfer chain or to O_2 via a plastid terminal oxidase (Carol and Kuntz, 2001). Similar to *psy*, expression of *pds* is under photosynthetic redox control in *H. pluvialis* (Steinbrenner and Linden, 2003), but is induced by blue light in *C. reinhardtii* (Bohne and Linden, 2002).

Following cyclization of lycopene the carotenogenesis pathway splits, forming the α- and β- branches of carotenes (Figure 8). Introduction of β-ionon rings at both ends of the linear lycopene molecule results in the formation of the symmetric β,β-carotene, termed β-carotene. This reaction is catalyzed by a single enzyme, lycopene β-cyclase (LCYB). The concerted action of LCYB on one side of the lycopene molecule and a second cyclase on the opposite end results in formation of β, ε-carotene, more commonly known as α-carotene. In most plants, the enzymatic capacity of the second cyclase, designated lycopene ε-cyclase (LCYE), is restricted to the introduction of a single ε-ionon ring per lycopene (Cunningham and Gantt, 1998). The α-carotene molecule is the precursor of lutein and loroxanthin, whereas violaxanthin, zeaxanthin, and neoxanthin are synthesized from β-carotene. The genes encoding both *lyc-β* and *lyc*-ε are nuclear and have been cloned from a number of vascular plants (Cunningham et al., 1996; Hirschberg, 1998). The encoded proteins share significant similarity and the genes probably evolved as a consequence of a duplication (Cunningham and Gantt 2001; Sandmann, 2002).

In photosynthetic tissues of vascular plants, the introduction of oxygen functions into carotenoids is limited to hydroxylations and epoxidations. Hydroxylation takes place at the C3-atoms of the ionon rings of both α- and β-carotene, resulting in the formation of lutein (β,ε-carotene-3,3-diol) or zeaxanthin (β,β-carotene-3,3-diol), respectively. The β-ionons can be oxidized by carotene β-hydroxylase (CHYB), a nonheme di-iron protein with four predicted trans-membrane helices (Bouvier et al., 1998, Sun et al., 1996). *H. pluvialis* is the only green alga from which a putative chy-β homolog was cloned, and the encoded protein was shown to be capable of hydroxylation of β-ionon rings as well as their 4-keto derivatives (Linden, 1999). Like the other carotenogenic genes, expression of chy-β from *H. pluvialis* is under redox control (Steinbrenner and Linden, 2001; Steinbrenner and Linden, 2003).

Violaxanthin is synthesized from zeaxanthin *via* the intermediate antheraxanthin by the stepwise introduction of epoxy-groups at the C5, C6 double bonds of the two ionon rings. Epoxidation by *zep* is restricted to *β*-ionon rings carrying a hydroxyl group at the C3 position (Bouvier et al., 1996). The *zep* gene from *C. reinhardtii* was identified by searching an EST library for clones encoding polypeptides with similarity to vascular plant *zep*; strains of this alga with point mutations in the *zep* gene were impaired in zeaxanthin epoxidation (Baroli et al., 2003). In vascular plants, violaxanthin de-epoxidase (VDE) catalyzes the reverse reaction of the ZEP enzyme, the de-epoxidation of violaxanthin to form zeaxanthin via antheraxanthin. Although not necessary for carotenoid biosynthesis, the reaction is part of the photoprotective xanthophylls cycle involved in the generation of hydroxy-carotenoids that function in the dissipation of excess absorbed light energy within the light-harvesting apparatus (Niyogi, 1999). The *vde* gene was identified in a number of vascular plants (Bugos et al., 1998, Bugos and Yamamoto, 1996; Emanuelsson, 2003; Zhang et al., 2003), and a VDE mutant of *C. reinhardtii* (npq1) was isolated by screening for mutants with reduced non-photochemical quenching (NPQ) (Niyogi et al., 1997). Loroxanthin, a xanthophyll present in *C. reinhardtii* but not in vascular plants, is derived from lutein by hydroxylation of the methyl group at C9 of the polyene chain (Britton, 1998). The mechanism of this reaction and the nature of the putative loroxanthin synthase (LSY) are not known. Surprisingly, although there are no reports on the presence of astaxanthin in *C. reinhardtii*, its genome contains an open reading frame with strong similarity to the carotene *β*-ketolase (BKT) from *H. pluvialis*; this enzyme catalyzes the introduction of keto groups at C4 and C4 of *β*-carotene as a step toward the biosynthesis of astaxanthin (Britton, 1998; Lotan and Hirschberg, 1995). This putative *bkt* gene is located next to *chy-β* and expressed since it is represented in cDNA libraries. A biochemical analysis of the protein product of this gene will establish whether it has ketolase activity or has acquired a different catalytic function.

1.2.7 Correlation between human health and photosynthetic compounds

Space ionizing radiations are one of the main limits to the permanence of biological organisms in space since they trigger the radical's formation potentially dangerous for all biological macromolecules. A direct correlation was observed between exposure to radiations and occurrence of DNA damages, cancer formation, cells apoptosis, skin and aging problems (Hellweg and Baumstark-Khan, 2007).

Also photosynthetic organisms are affected by the incident radiation even on Earth. When excess energy reaches the RC it is converted in fluorescence emission or dissipated trough heat in order to avoid oxidative damage (Govindjee, 1995). The generation of ROS is promoted when the photosynthetic machinery absorbs excess light or the availability of CO_2 or NADP is limited (Asada, 1996; 1999), result in an over reduction of the component belonging to the electron transport chain in the PSII protein complex.

The over-reduction lead to one-electron transfer to ground-state oxygen, producing the superoxide radical (O_2^-), hydrogen peroxide (H_2O_2), and the hydroxyl radical (OH).

At least three major sources of ROS production have been identified in photosynthetic systems; namely singlet oxygen from ^{3}Chl triplet states in the Light harvesting antenna complexes, superoxide anions and H_2O_2 from PSI reducing side in the absence of oxidized electron acceptors and charge recombination within PSII in the presence of reduced plastoquinone electron acceptors. Additional ROS species can be accumulated as secondary products of these major oxidants in the cell and by the Fenton reaction with metal ions. Carotenoids are the major resistance factors against oxidative stress in photosynthetic organisms where they act through distinct mechanisms in preventing ROS formation and scavenging the fraction synthesized despite the prevention effects. Recent work has revealed the specific role of carotenes and xanthophylls (oxygenated carotenoids) species in protecting against oxidative stress; namely, Neoxanthin was found to have a specific effect against superoxide anion (Dall'Osto et al., 2007), Lutein was shown to exercise a strong quenching effect on ^{3}Chl* thus preventing $^1O_2$ formation (Mozzo et al., 2008), while violaxanthin and zeaxanthin were shown to be effective in scavenging $^1O_2$, with a strong additional effect of zeaxanthin in quenching ^{1}Chl*, thus preventing ^{3}Chl* formation (Dall'Osto et al., 2010; Dall'Osto et al., 2007; Mozzo et al., 2008) .

Plants and algae are able to overcome the photooxidative damage actuating non-photochemical-quenching (NPQ) mechanisms involving dissipation energy trough heat, fluorescence emission and the quenching of single-excited chlorophyll.

The importance of different carotenoids was proved in *C. reinhardtii* by Niyogi KK and colleagues (1997) using the NPQ-mutant. In this work, mutants impaired in xanthophylls cycle are able to accumulate different xanthophylls products, for example the double mutant *npq2lor1* that accumulate zeaxanthin as the only xanthophylls component. Xanthophylls accumulation, like zeaxanthin, is sufficient to increase the resistance to photo oxidative damage (Baroli et al., 2003). Plants and algae are able to modulating their LHCII size depending to light quality and intensity. In dark conditions, photosynthetic organisms need efficient LHCII and increase antenna size, adjusting the ratio between carotenoids as

violaxanthin, antheraxanthin and zeaxanthin. The cyclic conversion of this carotenoids is called xanthophylls cycle. Under high light condition reduction of antenna size and accumulations of zeaxanthin was observed (Havaux et al., 2004). Indeed carotenoids biosynthesis is a crucial point in order to avoid photooxidative damage. Zeaxanthin and lutein are naturally produced in photosynthetic organisms when excess light is adsorbed, having an important role in quenching singlet oxygen and free radicals, protecting PSII apparatus and thylakoid membrane lipids from peroxidation (Baroli et al., 2003; Mendez-Alvarez et al., 1999). These pigments are mainly found in meat, and in the skin of fish, in the carapace of Crustacean, and in the subcutaneous fat, the skin, the egg yolks (primarily lutein, which is often added to feed increasing the yellow color), the liver, the integuments, and in the feathers of birds (poultry). Humans and animals in general are not able to synthesize xanthophylls *de novo*, compounds found in the blood or in various tissues are entirely of dietary origin.

The importance of these antioxidant compounds as diet supplement was proved in mouse, where systemic treatment with lutein, zeaxanthin, alpha lipoic acid, and reduced l-glutathione decreased oxidative DNA damage in rod photoreceptors and increased photoreceptor survival (Galbinur et al., 2009.). These pigments play an important role in slowing the age-related degeneration of these tissues, both directly as an antioxidant and indirectly by absorbing blue light (Santosa and Jones, 2005; Biesalski and Obermueller-Jevic, 2001).

The increasing concern about the importance of xanthophylls as oxidative stress reduction compounds with beneficial effects for human well-being brought to intensive research focused on regulation of genes involved in carotenoids biosynthesis as well as different strategies to increasing plants carotenoids production.

1.3 *Chlamydomonas reinhardtii*

The unicellular green alga *C. reinhardtii*, also known as "green yeast" (Goodenough, 1992; Rochaix, 1995), phylogenetically diverged from land plants over 1 billion years ago. It is a widely used model system for studying chloroplast-based photosynthesis, as well as the structure, assembly, and function of eukaryotic flagella (cilia), which were inherited from the common ancestor of plants and animals, but lost in land plants (Lefebvre and Silflow, 1999). Thanks to the availability of complete genome sequence (version 3.1), including chloroplast and mitochondrial genomes, annotated databases, high number of mutated strain and successful high-level expression of recombinant proteins in the chloroplast compartment (Mayfield et al., 2007; Manuell et al., 2007), *Chlamydomonas* (Figure 9) gained an increasing interest in cell biology studies, *e.g*. in the context of bio-fuel and hydrogen production (Grossman et al., 2007; Merchant et al., 2007).

Moreover, this unicellular alga is included in the group of organisms with a GRAS status (Generally Regarded As Safe), granted by the FDA, making it an interesting object of food and feed technologies studies, *e.g*. over-expressing foreign proteins with functional activity (antioxidant, colorant, provitamin or therapeutic properties).

Even the life cycle lead to a functional use of this organism, having a rapid growth in both liquid and solid media; a sexual cycle, that can be precisely controlled; genetic aspects which enable the generation and characterization of a wide collection of mutants with lesions in structural and metabolic regulator genes and a flexible metabolism being able to growth both phototrophycally and heterotrophycally (Grossman et al., 2003).

Growth and scale production of recombinant strains, using alternative methods instead of antibiotic resistance genes (Debuchy et al., 1989; Ferris, 1995) is possible in a reasonable time and the risk to contaminate the surrounding environment is excluded, because microalgae are not hosts to major pathogens, a huge problem when land plants are used (Ellstrand, 2001; Ellstrand, 2003; Ruf et al., 2007). The avoidance of antibiotic resistant gene to select mutants minimizes consumer's concerns about food safety and antibiotic resistance transfer.

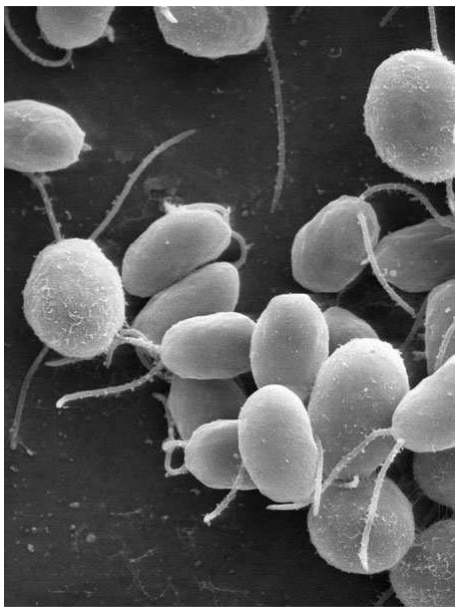

Figure 9. Scanning electron microscopy of *C. reinhardtii* cells (from http://www.miket.co.uk/latro.html).

1.3.1 *C. reinhardtii* NPQ mutants

A set of *C. reinhardtii* mutants carrying single and double mutation within carotenoid biosynthetic genes were included in this study (kindly provided by Prof Niyogi, University of California, Berkeley, Department of Plant and Microbial Biology, U.S.A.). These mutants (*lor1*, *npq2* and *npq2lor1*) are impaired in the biosynthetic steps that lead to the synthesis of xanthophylls and α-carotenes derivatives.

In particular, the lor1 mutant was generated by UV mutagenesis and selected for its phenotypical altered colour (Tellenbach, 1984). This mutant is defective in the lutein accumulation and its derivative loroxanthin; therefore, it lack the final product of the α-carotenes biosynthetic branch, while has a normal xanthophylls cycle (Chunayev et al., 1991; Niyogi et al., 1997b; Anwaruzzaman et al., 2004). After few years this mutant was characterized and a nonsense mutation (a single G/C-to-A/T base pair change) occurred within the third exon of the *lyc-ε* nuclear gene, encoding the chloroplast-localized enzyme lycopene ε-cyclase, LCYE was discovered (Anwaruzzaman et al., 2004).

The npq2 mutant was generated by insertional mutagenesis of the parental strain (CC-425) by plasmid transformation containing the wild-type ARG7 gene (Niyogi et al., 1997). The mutation impairs the zeaxanthin epoxidase activity, responsible for the conversion of zeaxanthin to antheraxanthin and violaxanthin. Consequently, the npq2 mutant accumulates zeaxanthin and lack antheraxanthin, violaxanthin and neoxanthin. The non-homologous recombination of the DNA plasmid with the nuclear genome of *Chlamydomonas* results in

random mutagenesis (Tam and Lefebvre, 1993; Davies et al., 1994) due to genes interruption or deletion. The inserted sequence could serves as a convenient tag to facilitate eventual isolation of the gene affected in the mutants (Tam and Lefebvre, 1993; Gumpel et al., 1995; Davies et al., 1996). *Arg+* transformants were grown photoautotrophically and identified using a digital video-imaging system with high light (1200 μmol photons m^{-2} sec-1), which excited chlorophyll fluorescence and induced NPQ (Niyogi et al., 1997).

The double mutant was obtained as a spontaneous npq2 mutant from the lor1 background (Chunayev et al., 1991; Niyogi et al., 1997a; 1997b). Thus, this *npq2lor1* double mutant lacks the lutein and loroxanthin as well as all zeaxanthin-derived xanthophylls (Polle et al., 2001).

All the aforementioned mutants were backcrossed at least four times to the *C. reinhardtii* cc-125 wild type (www.chlamy.org).

1.3.2 *C. reinhardtii* D1 mutants

A set of *C. reinhardtii* mutants carrying single mutations in the chloroplastic *psbA* gene, were produced and included in this study (in collaboration with Prof. Johanningmeier, Martin-Luther-University Halle-Wittenberg, Institute of Plant Physiology, Germany).

The D1 protein encoded by the *psbA* gene located in the chloroplast genome, is currently one of the most extensively studied thylakoid membrane proteins. Specific amino acids and functionally important regions in D1 are recognized to play a role in QB, herbicide, pigments and metal binding as well as in electron transfer reactions (Vermaas et al., 1991; Oettmeier W, 1992). During translation the protein is segmentally inserted into the thylakoid membrane (Kim et al., 1991) and translational regulation is mediated by specific proteins interacting with its mRNA at the 5' end (Danon and Mayfield, 1991). At the DNA level, the sequences of more than 30 *psbA* genes have been determined to date (Svensson et al., 1991). Of these, only *C. reinhardtti* (Erickson et al., 1984), *C. smithii* (Palmer et al., 1985), *C. moewusii* (Turmel et al., 1989) and *Euglena gracilis* (Karabin et al., 1984; Keller and Stutz, 1984) *psbA* genes are interrupted by introns. *C. reinhardtii* contains four large group I introns ranging in size from 1.1 to 1.8 kb.

A transformant with no introns in the *psbA* gene was obtained (Johanningmeir and Heiss, 1993) and represented the first example of the removal of a complete set of introns from a chloroplast gene. The newly generated strain is photosynthetically competent and contains no detecTable recipient genome copies. The loss of all four introns appears to be phenotypically silent.

A set of *C. reinhardtii* mutants carrying single mutations in the chloroplastic *psbA* gene, were included in this study (kindly provided by Prof. Johanningmeier, Martin-Luther-University Halle-Wittenberg, Institute of Plant Physiology, Germany).

The mutated strains were tested in space to select the ones showing the higher tolerance to Space environment. Following a synergetic approach, a series of experiments were also conducted in ground-based laboratories. A large number of strains were exposed to different ionizing radiations (*e.g*. neutrons, protons, HZE and gamma rays), simulating part of the complex radiation field present in space. The higher tolerance of the *C. reinhardtii* strains could be a result of an improved capacity of the organisms to counteract the action of reactive oxygen species (ROS) produced by the space ionizing radiations.

1.4 The FOTON-BIOPAN Space missions

A series of biological experiments were performed during Space missions Foton-Biopan by European Space Agency (ESA) between 1987 and 1999, studying the effects of microgravity and cosmic radiation on micro-organisms, on the embryogenesis of the stick insect, the radiation damage in plant seeds, bacterial spores and in plant tissues (http://www.spaceflight.esa.int/users/downloads/facilities-doc/Foton_exp.descPI_list.htm).

Foton is a Russian spacecraft (Figure 10), designed and built at the Samara Space Centre. The spacecraft consists of 3 modules – battery module, service module and re-entry module - of which only the latter is retrieved at landing. In October 2002 ESA organized a cosmic flight in Foton M1 housing a payload complement of 39 experiments in physical sciences, biology, fluid physics, exobiology, materials science and technology. The mission unfortunately exploded during the launch. In the near future, Foton-M2 and M3 were the next ESA's missions of this kind. Foton M2 and M3 capsules were launched in May 2005 and September 2007, respectively, aboard a Soyuz-U rocket from Baikonur Cosmodrome in Kazakhstan and spent approximately two weeks in Earth orbit. Among the others, the Foton M3 satellite transported also the Italian *Photo project*, a research of the MoMa project “From Molecules to Man: Space Research Applied to the improvement of the Quality of Life of the Aging Population on Earth” funded by European Space and Italian Space Agencies (ESA, ASI) MoMa combined the expertise of several researchers working in different research areas to study the reaction of living organisms to microgravity and cosmic radiation with a special attention to Aging and the Quality of Life (Ambesi, 2006).

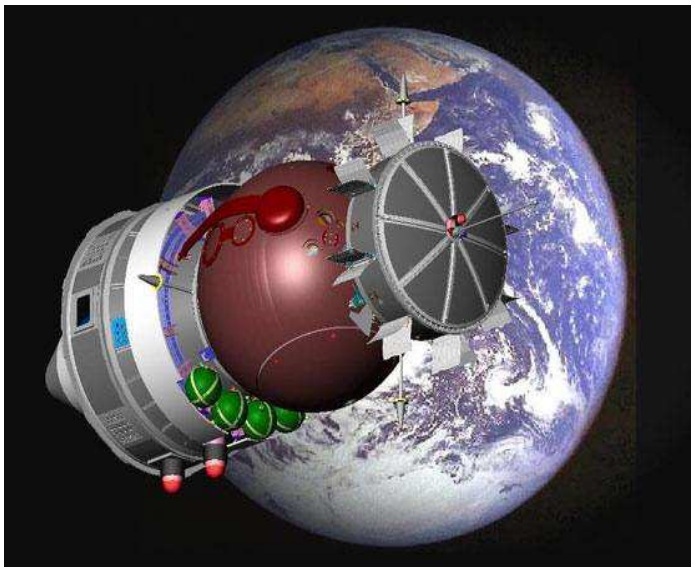

Figure 10 ESA FOTON- BIOPAN spacecraft.

1.5 STS-134 Space missions

The U.S. National Aeronautics and Space Administration (NASA) funded the Space Transportation System (STS) for the development and Shuttle operations. The Space Shuttle was a partially reusable launch system and orbital spacecraft operated on 135 missions from 1981 to 2011. The system was retired from service in July 8, 2011 after 135 missions, with Space Shuttle Atlantis performing that 135th launch - the final launch of the three-decade Shuttle program. The system combined rocket launch, orbital spacecraft, and re-entry space plane with modular add-ons. Major missions included launching numerous satellites and interplanetary probes, conducting space science experiments, and 37 missions constructing and servicing the ISS. Five space-worthy orbiters were built during these years, two were destroyed in accidents and the others have been retired.

The STS-134 mission was the last mission of the Space Shuttle Endeavour in which the Italian astronaut Roberto Vittori established an european record flying for the third time to the ISS (Figure 11).

Figure 11. Endeavour, STS-134 Space Mission 2011.

The STS 134 mission transported among the other, the DAMA project, sponsored by the ASI and the Italian Air Force (AM), a set of Italian experiments, namely the BIOKIS payload. The hardware required to make up the BIOKIS was entirely developed and manufactured by Kayser Italia (KI) a private SME aerospace system engineering company that features a long list of records in the field of Life and Physical Science investigations. The BIOKIS payload is made up by seven different experiments accommodated in two BIOKONs

(BIOKIS 001, BIOKIS 002), a KI standard transporTable containers for experiments processing (Figure 12).

A)

B)

Figure 12. The BIOKON containers flown aboard the STS 134 Mission. A) BIOKISS 001 carrying nDOSE and TARDIKISS experiments, **B)** BIOKISS 002 carrying BioSSPORE, Arabidops-ISS, PHOTOEVOLUTION, 3DISS, HiDOSE experiments (Vukich et al., *submitted*).

2 - AIM OF RESEARCH

The research activities reported in this thesis have been carried out in the context of Space Biology programs funded by ASI and ESA. The projects included the participation to Low Earth Orbit flight missions in collaboration with the Russian and NASA Space Agencies. The first mission, the Foton M3 satellite was launched from the Cosmodrome of Baikonur (Kazhakstan) at a height of about 400 km and the recoverable capsule returned to Earth after 12 days in orbit in 2007 (the Photo Project). The second flight, the STS 134 mission took off by the NASA's Kennedy Space Center to reach the ISS and lasted 16 days, in 2011.

These space missions represented an outstanding opportunity for the scientific community to embark on ambitious multidisciplinary researches in Space Life Science aimed to study life in the context of an extraordinary harsh environment.

The main objective of this thesis was to analyze the effect of the space environment on the physiology of the unicellular green alga *C. reinhardtii* focusing our attention on the photochemisty, molecular biology and analytical chemistry of photosynthetic process. The final aim was to provide an insight into some aspects of the tolerance of photosynthetic organisms to extreme environmental conditions.

Photosynthetic microrganisms represent a valuable resource as life regenerative supporting system in manned long-term space missions, being able to produce the oxygen necessary for atmosphere revitalization, food and nutraceuticals for human consumption. The exploitation of oxygenic photosynthetic microalgae is particularly suited to this purpose, because algae are characterized by high photosynthetic performance, minimal nutritional requirements and rapid accumulation of biomass with considerable nutritional value. In addition, their cultivation can be easily controlled in photobioreactor, it is not season-dependent and demands less volume for growth compared to land-plants.

Specific objectives of this thesis included the characterization of the *Chlamydomonas* D1 mutants after their return on earth in terms of photosynthetic electron transport efficiency, accumulation of antioxidant compound occurring in the photosynthetic apparatus, expression analyses of the main genes involved in carotenoid and plastoquinones/tocopherols biosynthetic pathways. In parallel, the set-up of on-ground control experiments was planned in order to rule out effects not due to the space environments.

The activities carried out during the first 18 months of this thesis regarded the characterization of the strains flown aboard the Foton M3 satellite. Later on, the main efforts

regarded the organization and participation to the DAMA mission, a fleet of Italian experiments in which the BIOKIS payload including our experiment PHOTOEVOLUTION, experienced the space environment on board the Space Shuttle docked to ISS. PHOTOEVOLUTION aimed to test the capability of previously and new obtained site-directed *Chlamydomonas* strains to deal with the space environment and, again, to unravel the molecular mechanisms underlying their improved tolerance.

All the studies developed in this thesis aim to select life regenerative supporting systems suiTable for long-term space missions onboard the ISS and/or manned missions to Moon and Mars.

3 - MATERIALS AND METHODS

3.1 *C. reinhardtii* culture conditions

C. reinhardtii stock cultures were maintained at 25 °C on agar plates prepared with Tris-acetate-phosphate (TAP) medium (Harris E., 1989) under continuous illumination (~50 µmol m^{-2} s^{-1}). Liquid cultures were similarly grown but on TAP liquid medium with agitation at 150 *rpm*. All experiments were carried out on cell cultures in the mid-exponential growth phase.

3.2 *C. reinhardtii* D1 mutants production

The main *Chlamydomonas* strains exploited were IL, a mutant containing an intronless *psbA* gene (Johanningmeier and Heiss, 1993) that represented the control parent strain for characterization of the D1 mutants, and Del1 mutant (Preiss et al., 2001), used as a recipient strain for D1 mutants generation. Del1 is a derivative of the IL parent strain lacking an approx 0.4 Kb fragment encoding amino acids Ala153 to Ala294 of the PSII D1 protein. As a result of the deletion, the strain synthesizes a truncated D1 protein and is able to grow only mixotrophically on TAP medium using acetate as a carbon source. Because of this, the acetate-free high-salt (HS) medium was used as a selection pressure for photoaoutotrophic growth. The photoautotrophically incompetent Del1 strain can be transformed by particle gun bombardment with PCR-generated *psbA* fragments, resulting in colonies able to grow photoautotrophically on HS medium (Dauvillee et al., 2004).

3.3 Site-directed PCR-based mutagenesis

Site-directed mutagenesis was performed by a two-steps PCR procedure using as a template the pSH5 plasmid containing the complete intronless *psbA* gene and the 3'-flanking region (Dauvillee et al., 2004; Figure 13). In the first step, two DNA fragments, upstream and downstream from the position of the target point mutation were synthesized (for example in the case of I163T mutants, the one corresponding to position 163 in the D1 protein). Using the I163T mutant as an example for the synthesis of the upstream fragment, an outer forward primer and 163-reverse primer, which starts at the codon in the *psbA* gene that corresponds to position 162 in the D1 protein, were used. Similarly, for the downstream fragment a 163-

forward primer, which starts at the codon in the *psbA* gene that corresponds to position 164 in the D1 protein and an outer reverse primer were utilized. PCR amplicons were analyzed by agarose gel electrophoresis, extracted and purified using the commercial kit SV Gel and PCR Clean-Up System (Promega, USA). The purified DNA fragments were used in the second PCR in the presence of the two mutagenic primers, hosting the target mutation, together with the outer primers from the first PCR.

The pSH5 plasmid was amplified in a total volume of 50 µl containing 100 ng plasmid DNA, 5 µl 10x Taq-polymerase buffer, 3 µl of 25 mM $MgCl_2$, 5 µl of 2 mM dNTPs, 20pmoles of each primer and 1 unit Taq-polymerase using Trioblock (Biometra) and using the primers as mentioned in **Table 4.** The standard PCR protocol used was: 25 cycles of 94°C denaturation (1 min), 52 °C annealing (1 min), 72 °C extension (2 min) with a 5-min denaturation step at 94 °C in the first cycle and a 10-min extension step at 72 °C in the final cycle.

The fragments obtained from the second PCR were analyzed and the amplicon of interest was purified and amplified in subsequent standard PCR. This mutated amplicon was directly used for the algal biolistic transformation (Dauvillee et al., 2004; Figure 13).

After cell re-growing, a single colony was picked from a bombarded filter and was transferred to HS liquid medium. The point mutation was verified by *psbA* gene sequencing (Seqlab, Göttingen, Germany). The homoplasmicity of the *psbA* mutant was verified by standard PCR and agarose gel electrophoresis. Only homoplasmic colonies were used in all the described experiments.

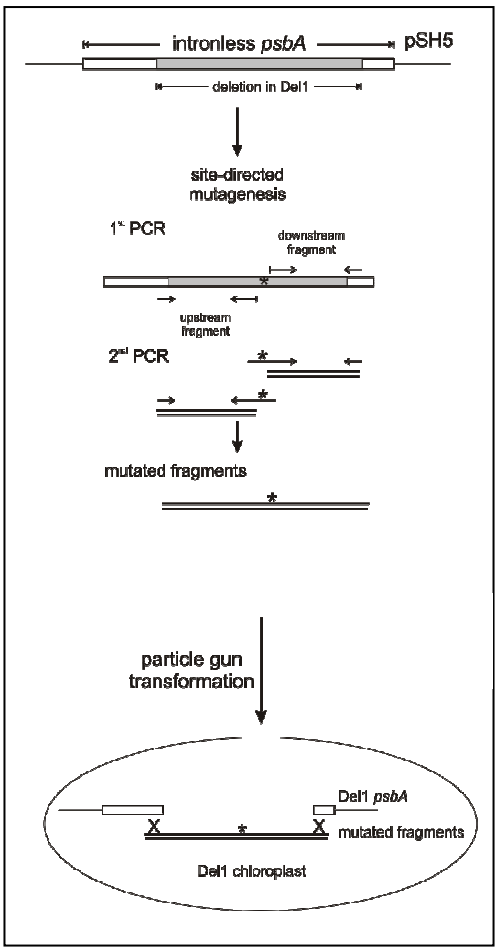

Figure13. PCR-based mutagenesis for introduction of site-directed mutations in the *psbA* gene of *C. reinhardtii*, coding for the D1 protein of PSII core complex. Two-steps PCR with mutagenic primers was performed, using as a template intronless *psbA* gene in vector pSH5. The PCR fragments were precipitated directly onto tungsten particle and were introduced in to the recipient strain by particle gun, without further cloning or purification. The homologous recombination in the recipient Del1 strain is indicated by crosses. The primers are represented as arrows and the stars indicate point mutations. The shaded area in the *pbs*A gene indicates the deletion region in the Del1 mutant.

1st PCR		2nd PCR	
Primers	**Sequence (5' → 3')**	**Primers[a]**	**Sequence (5' → 3')**
outer for	GGTGCTGTAATCCCAACTTCT		
outer rev	CTAGAGTTAGTTGAAGCTAAGTCTAGAGGGA		
I163 rev	AGGGTAAACTAAGAATACAGC	**I163Tmut-rev**	CTTAGTTTACCCT**ACC**GGCCAAGGTTCATTCTCTG
I163 for	GGCCAAGGTTCATTCTCTG	**I163Tmut-for**	GAACCTTGGCC**GGT**AGGGTAAACTAAGAATACAGC
P162rev	GTAAACTAAGAATACAGCTGAAGC	**P162S mut rev**	GAACCTTGGCCGAT**TGA**GTAAACTAAGAATACAGCTGAAGC
P162for	ATCGGCCAAGGTTCATTCTC	**P162S mut for**	CTGTATTCTTAGTTTAC**TCA**ATCGGCCAAGGTTCATTCTC
L200rev	CATGTGGAATGGGTGCATAAG	**L200I mut rev**	CACCAGCAACACC**AAT**CATGTGGAATGGGTGCATAAG
L200for	GGTGTTGCTGGTGTATTCG	**L200I mut for**	CACCCATTCCACATG**ATT**GGTGTTGCTGGTGTATTCG
I281rev	TACCGGCCAAGCAGCTAAG	**I281T mut rev**	GTGAACCAAATACC**TGT**TACCGGCCAAGCAGCTAAG
I281for	GGTATTTGGTTCACTGCTTTAG	**I281T mut for**	GCTGCTTGGCCGGTA**ACA**GGTATTTGGTTCACTGCTTTAG
G207rev	GAATACACCAGCAACACCTAAC	**G207S mut rev**	CTGAGAATAATGAACC**TGA**GAATACACCAGCAACACCTAAC
G207for	GGTTCATTATTCTCAGCTATGC	**G207S mut for**	GTGTTGCTGGTGTATTC**TCA**GGTTCATTATTCTCAGCTATGC
M172rev	ACCGTCAGAGAATGAACCTTGG	**M172L mut rev**	CAGAGATACCTAAAGG**TAA**ACCGTCAGAGAATGAAC
M172for	CCTTTAGGTATCTCTGGTAC	**M172L mut for**	GTTCATTCTCTGACGGT**TTA**CCTTTAGGTATCTCTG

Table 4. Sequences of primers used in the two-step PCR for the site-directed mutagenesis. [a]The modified nucleotides in the mutagenic primers are indicated.

3.4 Foton M3: flight and ground-control samples preparation

Flight and ground-control samples were prepared producing small volumes of high-density cell cultures that were subsequently enclosed into the modular multifluorescence device, specifically developed for the space mission (**Figure 14**). This device includes small containers (biocells) to accommodate the selected algal cells. Before samples preparation, the biocells were sterilized and filled in with TAP agar (1.65%) medium. Algal cells in liquid cultures at the mid-exponential growth phase were harvested by low speed centrifugation, re-suspended in 150 µl of TAP medium to A_{750nm} = 9 and layered on the TAP agar medium poured off into the biocells. After cells adsorption (approx. 30 min.), the biocells were hermetically closed under sterile conditions and mounted in the multicell fluorescence sensor. The experimental device was sent into space as described below. After returning from the space flight, the multicell fluorescence sensor was shipped to our laboratory on day 3 after landing. The first set of sample was immediately opened under sterile conditions and the algal strains transferred to liquid TAP medium. The second set of modules was opened on day 15 after landing and treated as the first set. In both cases, the cell cultures were re-grown in liquid medium for three days in order to reach a mid-exponential growth phase and then analyzed.

3.5 The multicell fluorescence sensor: in-flight monitoring of chlorophyll *a* fluorescence induction

The multicell fluorescence sensor named Photo II was designed by Biosensor.srl (Formello, Italy; www.biosensor.it) and comprised 12 arrays of 2 or 3 biocells (20x10x5 mm) each allowing for simultaneous analyses (Cano et al., 2011; **Figure 14**).

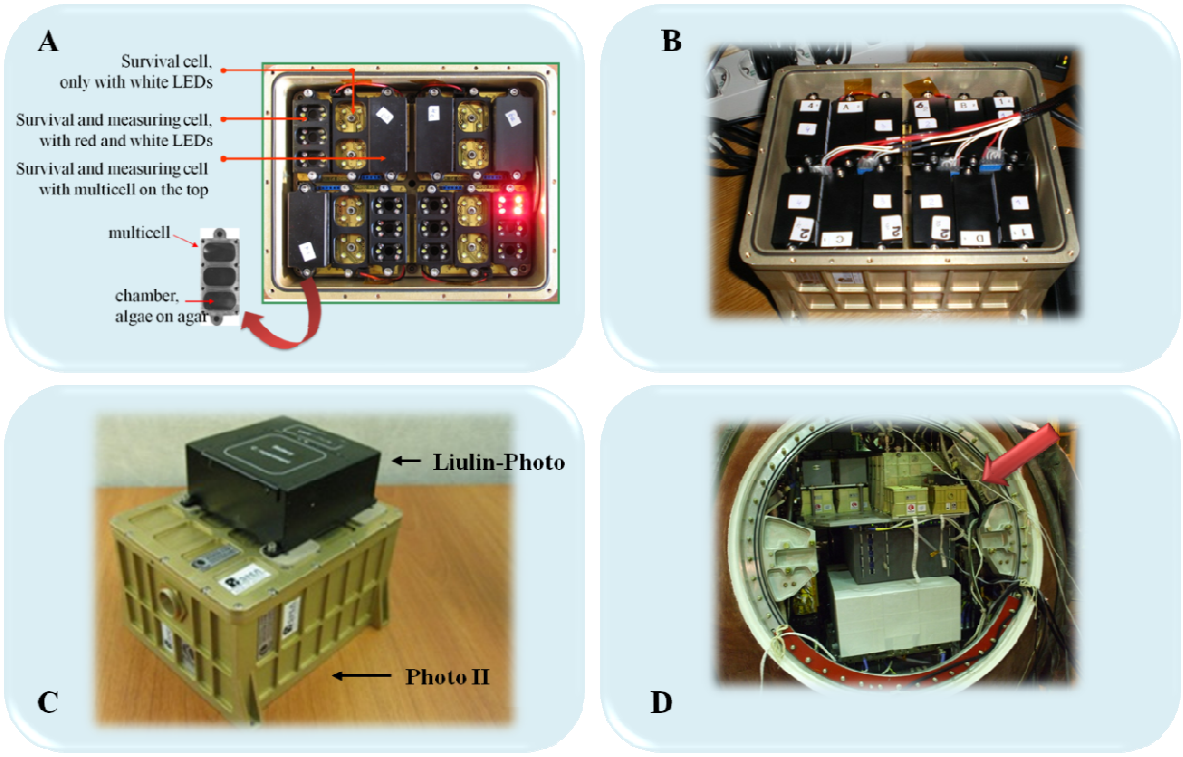

Figure 14. Overview of the Photo II payload docked into the Foton M3 satellite. A) Top view of the Photo II device with indications of the associated electronic components. The red LEDs pulse with peak at 660 nm and 6s duration, the white LEDs provide actinic light 7/17h light/dark period. **B)** Top view of the assembled Photo II device hosting the biological samples, enclosed in the BIOKON (Kayser Italia). **C)** Photograph of the complete Photo II experiment equipped with the spectro-dosimeter Liulin before the integration in the re-entry module of the Foton M3 satellite. **D)** Frontal view of the opened re-entry module of the Foton M3 satellite indicating the position of the Photo II-Liulin assembly (red arrow).

Modularity and configuration were implemented through separation of each cell into two independent sub-modules: a fixed bottom section which accommodated the optical devices and a removable upper section containing the sample that was disposed off after testing and replaced by a new one for fresh analysis. Two red (650 nm) LED excitation light sources and a fluorescence emission photodiode detector were mounted in each cell. Each photodiode was coupled to a different interference band pass filter, tuned to the desired fluorescence intensity peak. The photo-generated output current was amplified and converted into a voltage signal by a read-out electronic circuit, coupled to an electronic control board driving the LEDs on/off by a programmed timer. Each photosynthetic sample was provided with two additional white LEDs, mounted close to the exciting ones, and grown under repeating cycles of 7h light/17 h darkness using a timer. In this way, long-term measurements were made possible. The light intensities of all LEDs were controlled and set electronically. Measured data were stored onboard through 12-bit resolution sampling at 480 KHz and ADC conversion, in a flash memory card from which information was constantly retrievable. The

multicell fluorescence sensor was equipped also with four solid-state temperature sensors that provided temperature values for each fluorescence measurement. Internal batteries (8.2-7.3 V) were the power source. Total weight of the equipment (dimension 100x100x150 mm) without batteries and external case was 0.25 kg. The instrument allowed simultaneous determination of the following chlorophyll fluorescence parameters: F_0, F_m, F_v, the ratio F_v/F_m, the area over the fluorescence curve, and the time to reach F_m in each sample. F_0 was calculated by using an algorithm that determined the line of best fit for the initial data points recorded at the onset of illumination; the best-fit line was then extrapolated to time zero to determine F_0 (Tsimilli-Michael and Strasser, 2008**).**

3.6 The space environment during the Foton M3 mission: radiation and temperature conditions

The space radiation data were collected by a porTable, active spectrum-dosimeter Liulin-Photo on board the Foton M3 satellite and analyzed **(Figure 14).** No unusual energetic phenomena (such as flares and coronal mass ejections) were recorded on the Sun during these periods, neither did geomagnetic storms occur. The total dose measured on the detector was 1.85 ± 10% mGy. The inner Van Allen radiation belt (South Atlantic magnetic Anomaly, SAmA) crossovers were characterized by dose and flux peaks as high as 292 ± 10% mGy h^{-1} for Liulin-Photo. Peaks were due to trapped protons with energy up to 300–400 MeV. Relativistic electrons in the outer radiation Belt were not recorded since Liulin-Photo was behind a high shielding that did not allow the trapped electrons to penetrate. Over a narrow region in the centre of the SAmA, characterized by the highest dose peaks, the average dose spectra showed that, in R3D-B3, the maximum dose was deposited by 66 MeV protons. A detailed analysis of the energy spectra corresponding to the SAmA transits indicated that the Foton capsule provided an effective shielding against free-space protons with energy E<w130 MeV (Damasso et al., 2009).

The temperature was measured during the entire duration of the experiment by termocouples included in the Photo II device.

3.7 The PHOTOEVOLUTION experiment: sample preparation and immobilization in the PHOTOI device

PHOTOEVOLUTION is one of the 7 experiment included in the BIOKIS payload flown on the STS 134 mission enclosed in the BIOKON002.

C. reinhardtii I163N, I163T and P162S D1 mutant and the IL parent strains were grown in TAP liquid medium to reach the early exponential growth phase. Cell cultures were hence harvested by weak centrifugation (3000 *rpm* x 5 min), resuspended to obtained a final OD750=2 and layered on 300 µl of 1.65% TAP agar medium previously solidified in the biocell of the PHOTOI device (Figure15). The Photo I is a passive container specifically designed by the Kayser Italia Company for space science. It consists of a plastic body having sixteen wells hosting the biological materials and a transparent inner cover allowing the photosynthetic reaction of the enclosed samples. Each well is provided of an O-ring important for the hermetic closure of the instrument, avoiding contamination and excess over dray of the solid media.

After cell culture immobilization, PHOTOI was hermetically closed by two covers (Figure 15). The PHOTOI was hence enclosed in the BIOKON 002 (Figure 16) and sent to the Kennedy Space Center.

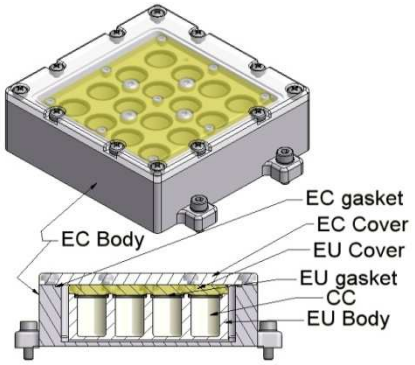

Figure 15. Schematic representation of PHOTO I experiment unit developed into the frame of the DAMA mission (2011).

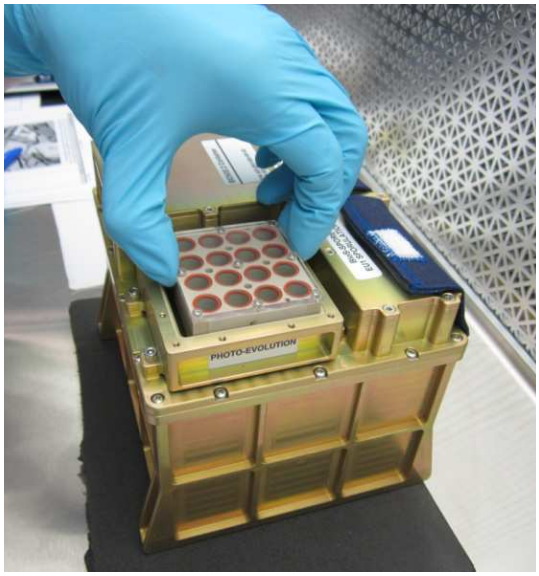

Figure 16. Photo I experiment integration into the BIOKON before the STS 134 Endeavour spacecraft take off.

3.8 Chlorophyll *a* fluorescence induction

In on-ground experiment, photosynthetic performance was assessed by chlorophyll fluorescence measurements using the Fluorescence Monitoring System (FMSII, Hansatech, King's Lynn, Norfolk, UK). Fluorescence activity was recorded at every critical step of the experimental procedure: i) arrival at the Kennedy Space Centre-NASA, ii) before the launch iii) after landing and iv) at the arrival at the principal investigator laboratory.

The fluorescence emission was measured at room temperature for 2.5 s, the duration of the saturated pulse was 0.7 s. The values for the minimal (*Fo*) and the maximum (*Fm*) fluorescence are automatically calculated by the instrument. Prior to each measurement, the samples were kept in dark for 10 min in order to reach PSII dark-adapted state that is required for the registration of the real *Fo* (corresponding to the fluorescence from open reaction centres). After illumination with saturated white light pulse, the fluorescence signal increases up to its maximum, *Fm*, as a result of reduction of Q_A, the primary quinine acceptor of PS II-fluorescence from closed reaction centres. Only the reaction centres which are able to reduce QA (*i.e.* photochemically active reaction centres) can contribute to the variable fluorescence yield, *Fv=Fm-Fo*.

3.9 Functional characterization of the site-directed mutant strains under saturating light condition

The oxygen evolution capacity of the selected strains was measured on TAP liquid cell cultures, containing 15±2 mg l^{-1} chlorophyll, at 24°C using a Clark-type oxygen electrode (Chlorolab 2, Hansatech, Instr. Ltd, Norfolk, UK) in the presence of 10 mM $NaHCO_3$ as an additional carbon source (Melis et al., 1999). Samples were illuminated with increasing light intensities provided by red LEDs (660 nm) under continuous stirring. The rate of oxygen evolution under each of the light conditions was recorded continuously for a period of 2 min.

3.10 RNA extraction and Real Time PCR

Chlamydomonas culture at OD_{750} 0.4 were harvested by centrifugation (at 4°C for 10 min at 4500 *rpm*) and the cell pellet was suspended in 2 ml of DEPC-treated extraction buffer (50 mM Tris-HCl (pH 8), 0.3 N NaCl, 5 mM EDTA and 2% w/v of sodium dodecyl sulphate). Proteinase K solution (40 µg/ml final concentration) was added and the samples were left at room temperature for 15 min, 250 *rpm*. The resulting cell lysate was extracted

twice with phenol:chloroform (1:1) (phenol chloroform equilibrated to pH 4.3, Sigma), and RNA was precipitated overnight in 2 volumes of 100% EtOH. The precipitate was washed once with 70% EtOH and finally dissolved in 40 µl of RNase-free water. The quality of RNA was checked loading 500 ng onto a 1.2% formaldehyde-agarose gel, and, after quantification by NanoDropTM Spectrophotometers (Thermo Scientific, Wilmington, USA), DNase treatment was performed (RQ1 DNase 1U/µl, Promega) incubating 30 minutes at 37°C. The samples were extracted with phenol:chloroform (1:1) (phenol chloroform equilibrated to pH 4.3. Sigma), and RNA was precipitated overnight adding LiCl (4M final concentration) in H_2O DEPC and 2.5 volumes of 100% EtOH at -80°C. The precipitate was washed once with 70% EtOH and finally dissolved in 20 µl of RNase-free water.

RNA samples were reverse transcribed and amplified using the KAPA SYBR FAST Master Mix (2X) ABI Prism (Kapa Biosystems) and MuLV Reverse Transcriptase Reagents (Applied Biosystems), following the one-step RT-PCR protocol recommended by the manufacturer. About 100 ng of mRNA in 25 µl SYBR Green PCR Master Mix 1X with 0.25 U/ul MuLV Reverse Transcriptase (Applied Biosystems), 100 nM forward and reverse primers (Table 5), were subjected to the following thermal profile: one step at 42°C for 30 min, one step at 95 °C for 3 min, 40 cycles with a denaturation step at 95 °C for 3 s and an annealing/extension step at 60 °C for 20 s. PCRs were performed in the Real Time Step One Plus instrument using Frame Star Fast Plate, 96 well semi skirted, clear frame (ABI Fast Plate) and QPCR adhesive clear seals (Kapa Biosystems). The reactions were subjected to a heat dissociation protocol present in the Real Time Step One Plus software for melting curve analysis and detection of non-specific amplifications: at the end of the final PCR cycle, the amplification products were heat denatured over a 35 °C temperature gradient at 0.03°C/s from 60 to 95 °C. A negative control without template was run with every assay to assess the overall specificity. For each gene, a common threshold setting applied to each of the two biological replicates determined the threshold cycle (CT). Relative abundance of each gene was determined by the $2^{\Delta DDCt}$ method (Livak and Schmittgen, 2001). *Rack*1 (Schloss, 1990) was used as the endogenous control for calculation of relative abundance. Each assay included duplicate reactions. Primers design and their optimization in regard to primer dimer, self-priming formation and primer melting temperature was done with a melting temperature of 59°–60°C and a product size between 90 and 150 bp; were designed using Primer 3 software (http://frodo.wi.mit.edu/primer3/).

Gene	Primer sequence (5'→3')	Amplified fragment size (cDNA bp)	*C. reinhardtii loci*	*A. thaliana* orthologous
psy	TGGATGAGCTGGACAAGT GTCCGTGAAGTATTGCCG	140	AY604702	At5g17230
pds	ACCATGACTGAGCTGGAG CTTGTACTTGCGGATCTTGG	78	XM_001690807	At4g14210
lycβ	TGACGCTGTTCTGGAAGA CTCCTTGAGCGACATTGT	140	AY860818	At5g57030
vdr1	CCTTCTACTTGTCGGTATTGG TTCTCATCGCAGTCCACA	73	XM_001694990	n.d.
hst1	ACCAGCCTCTACACCTTT TGTACACGCCGAAGTTGA	136	XM_001695289	n.d.
mpbq-mt	CACCCCTACTTCATCTCCAT GTGTTCTTGTTCCAGTCCTC	95	XM_001692671	n.d.
psbA	ACACTTGGGCAGACATCA AGGGAAGTTGTGAGCGTT	77	NC_005353	AtCg00020
psbD	TGCACCGTGTAAAGCAAC GCTGTTTCTACACCTGCTAAC	129	FJ436959	AtCg00270
rack1	TGCAAGTACACCATTGGC CCAGACCTTGACCATCTTGT	123	XM_001698013	n.d.

Table 5 Specific primers, amplified fragments size and primers concentration used for gene RT–PCR analysis. Orthologous genes from *Arabidopsis thaliana* are also reported.

3.11 Quantitative and qualitative analyses of photosynthetic pigments

3.11.1 Pigment standards and HPLC system

All standards (carotenoids, xanthophylls and chlorophylls) were bought with the highest purity. All other chemicals and solvents were HPLC or ACS grade (Carlo Erba, Milan, Italy).
All the pigment standards were prepared at the suiTable concentration for the necessary calibration of HPLC curves, by diluting the stock standards solution under dim (or green safe) light and at 4°C. Nitrogen gas was flushed into vials to avoid pigments degradation and isomerization. All the vials were stored at –20°C and in the dark. The HPLC instruments (Gilson, Milan, Italy) encompass a gradient system (two 306 pump, 811c dynamic mixer, 805 manometric module, 155 UV/Vis detector) and a Rheodyne mod 7125 injection valve (20 µl loop). The HPLC system and the chromatographic data were controlled by a 506 interface (Gilson) from the Unipoint Gilson software. The HPLC column was an YMC C30 column (Waters, USA), 5 µ, 250 x 4,6 mm id, plus a C18 (1 cm) guard column and in-line filter (0,22 µm). Both the HPLC and the guard columns were thermostated by the "Croco-Cil" HPLC column heater (Sainte-Foy-la-Grand, France).
Standards were diluted/dissolved in degassed 100% iced acetone in amber vials at stock concentrations under Nitrogen flux (GC grade), and dim lights. Stocks were kept frozen at –20°C. Working standard solutions were diluted with the HPLC solvent mixture methanol-acetonitrile-water (84:14:2, v/v/v) (solvent A) to avoid solvent interference during the run. We chose the solvent A, after different tests, because it showed the best peaks resolution. The HPLC calibration curve of each standard was analyzed at least three times. No by-products in the standards were detected by HPLC analyses for a period of at least three months.

3.11.2 Carotenoids and chlorophylls extraction

C. reinhardtii cultures of flown strains, after re-growing in physiological conditions up to $OD_{750} \approx 0.3$ in liquid TAP medium, were collected (15 ml) and centrifuged for 15 min at 4°C at 3500 *rpm*. Then the growth medium was discarded and samples immediately frozen at -80°C. Subsequently, samples were thaw on ice and lyophilized at -50°C under vacuum overnight. The exact dry weight of each sample was measured to normalize all samples on mg dry weight basis. A small amount of HPLC grade water (200 µl) was added to allow the next extraction steps. Re-hydrated samples were supplemented with some crystals of Na-carbonate to avoid a drop of the pH due to the lyses in the sample; immediately after, samples were re-suspended in 100% cold acetone. After vortexing and centrifuging (15 min at 4°C at 3500

rpm), samples were re-suspended in 1 ml of 100% cold acetone or until the pellet was bleached. Before HPLC injection, solutions were filtered through a 0.45 µm PVDF filter and dried under N2 bubbling. Hence, extracts were diluted with 400 µl of a mixture composed by solvent A and placed in amber vials. Samples were stored at -20°C until analysis.

3.11.3 Pigments analyses

Each 20 µl injection was performed by the "full loop" technique and each sample was analyzed almost three times (3 independent runs). When necessary for confirmation, standards were added to the sample extract for co-chromatography.

The most suiTable mobile phase system comprised a mixture of solvent A and 100% methylene chloride (solvent B) with the following gradient condition [time (%A, %B)]: [10 (100, 0)], in 10 min [10 (95, 5)], in 15 min [10 (80, 20)], in 10 min [5 (50, 50)], in 5 min [10 (100, 0)]. The flow rate was 1.0 ml/min. Pigment detector was set at 440 nm (carotenoids and xanthophylls) and 640 nm (chlorophylls). The column temperature was maintained at 21°C.

The HPLC column was an YMC C30 column (Waters, USA), 5 µ, 250 x 4,6 mm id, plus a C18 (1 cm) guard column and in-line filter (0,22 µm). Both the HPLC and the guard columns were thermostated by the "Croco-Cil" HPLC column heater (Sainte-Foy-la-Grand, France).

4 – RESULTS

4.1 The Foton M3 Space Mission: previous results from the Photo Project

The *Photo project* investigated the possibility of using oxygenic photosynthetic microorganisms for long-term Space flights as a source of oxygen, food and nutraceutical compounds. The goal pursued was to assess the effects of the space environment on various mutated microorganisms in order to select resistant-tolerant strains and determine the production of compounds with antioxidant properties resistant to space ionizing radiation.

Nevertheless, algae are not naturally adapted to the harmful space environment and the obtaining of novel strains with improved capability to cope with extreme conditions, such as the presence of high energy particles and ionizing radiation, was the starting point of these studies. By exploiting an in vitro directed evolution strategy targeted to the photosynthetic reaction centre D1 protein, a huge library of *C. reinhardtii* mutants was produced in our laboratories. Radiation-tolerant strains were selected after exposure of the random mutant library to proton or neutron sources. Some of these strains experienced the space environment aboard the Foton M3 satellite enclosed into the specifically developed Photo II fluorometer. The device hosted also the NPQ *Chlamydomonas* mutants, in order to check if a higher accumulation of antioxidant pigments could account for a possible improved space tolerance.

On return on earth, the algal strains immobilized into the Photo II device were cultured in both liquid and solid media and tested for their reproduction capability and stress recovery capacity. In parallel, ground control experiments were set-up reproducing immobilization times and temperature conditions experienced during the entire duration of the *Photo project*. Because the first analyses carried out on the flown algae indicated the occurrence of contaminated strains and/or strains unable to tolerate the specific immobilization conditions, subsequent analyses focused on a set of 5 mutants. The obtained results indicated that the space conditions did not modify cell viability of the analyzed strains. All the strains, were able to re-grow in liquid medium restoring flagella and motility (lost during the flight) and recovered the damage activating specific strain-dependent mechanisms (G. Rea personal communication).

In this thesis, a deep characterization of photosynthetic performance, photosynthetic pigment accumulation profiling and carotenoid biosynthetic gene expression pattern were carried out to gain further insights in the characterization of the acclimation mechanisms adopted by *C. reinhardtii* strains to the space environmental conditions.

4.1.1 Analysis of Photo-II fluorescence data of Foton M3 Space mission

The missions took place during periods of a quiet solar activity in the minimum phase of the 23rd solar cycle. The temperature during the flight missions and prior to entry and analysis on ground, measured by the fluorescence sensor, varied between 15-21 ± 2°C (Figure. 17).
During the mission, the passive dosimeter measured the contribution of protons in terms of Dose Ray corresponding to 10÷100 μGy h^{-1} (Damasso et al., 2009).
Analysed mutants included the intronless parent strain IL, its derivative D1 mutants A251C (near the Q_B binding pocket) and I163N (in the environment surrounding Tyr 161) and the abovementioned wild-type cc125 and npq2lor1 double mutant (Table 6). It is interesting to note that mutants have a lower Chl content compared to the parent and wild-type strains, while the photosynthetic performance is not significantly modified.

Strains	Mutation amino acid substitution or insertion in D1	Chlorophyll* (μg/ml)	Fv/Fm**
IL	*psbA* gene without introns	10.8 ± 2.5	0.810 ± 0.005
I163N	*Ile163* → *Asn* near to Tyr 161, the primary electron donor of P680. Obtained under neutrons	5.4 ± 1.1	0.799 ± 0.005
A251C	*Ala251* → *Cys* in binding niche for Q_B Resistant against different class of herbicides	5.1 ± 0.9	0.752 ± 0.006
CC125	Wild type (www.chlamy.org)	10.8 ± 2.2	0.813 ± 0.004
npq2	Impaired in the conversion of zeaxanthin in antheraxanthin	10.7 ± 2.1	0.731 ± 0.008
lor1	Unable to make α-carotene, lutein and loroxanthin because it is defective in ε-cyclase	9.4 ± 1.0	0.779 ± 0.010
npq2lor1	Accumulation of zeaxanthin and β-carotene	6.3 ± 0.9	0.715 ± 0.008

Table 6 Main characteristics of D1-mutants of *C. reinhardtii* selected for the flight.
*the chlorophyll content was calculated for algae suspension in logarithmic growing phase, OD=0.35, ± SE, n=3.
**the values for Fv/Fm were measured in medium used for multicells preparation, ± SE, n=9

The algae were sent in space enclosed in the Photo II device that, as previously described in Material and Methods, is capable to measure the chlorophyll fluorescence induction curve in photosynthetic organisms and provide the living conditions essential for the survival of the biological samples by photoperiodic day/night cycles.

Fluorescence was recorded hourly during the 7/17 hours light/dark photoperiod for 5 days before flight, 12 days during the flight and 10 days after landing. Detailed analyses of the daily trend in the maximal quantum yield of PSII photochemistry as F_v/F_m ratio, allowed to estimate the ability of the different *C. reinhardtii* strains to maintain their photosynthetic electron transport during the flight and after the landing. The results for both flight and ground control experiments are reported in Figure. 17. The photochemical efficiency of the flown parent strain IL remained sTable during the flight, while daily and gradually declined after landing, reaching a total decrease of Δ=0.05 F_v/F_m on the last day of the experiment. In the corresponding IL on-ground control, F_v/F_m values were unaffected during all the analysed days, indicating that the modification observed in the flown samples were not due to the immobilised condition experienced in the device, but to the space environment. Interestingly, the mutant strains I163N and A251C maintained a sTable photosynthetic activity not only in flight, but also after landing, showing a negligible decrease compared to the respective ground control samples, leading to hypothesise an increased capability to cope with the space environment. Similarly, the double mutant *npq2 lor1* showed a very sTable photosynthetic efficiency for the entire duration of the experiment reporting a negligible decrease of F_v/F_m ratio. A different behaviour was observed in the cc125 wild type, in which the F_v/F_m recorded during the flight was sTable, but dramatically declined after landing showing a decrease of Δ=0.23. These results provided the primary indications that space environment negatively affect the parental IL and wild-type cc125 strains, while the mutants I163N, A251C and *npq2 lor1* demonstrated a more efficient acclimation response.

In order to gain further insights into the previously obtained results, a detailed analyses have been performed on the chlorophyll a fluorescence-rise. At room temperature, the fluorescence transient of dark-adapted samples induced by saturating light intensity, displays a polyphasic rise with two intermediate steps appearing between the minimum yield (*O*) and the maximum yield (*P*) called J and I, the so called OJIP transient (Strasser et al., 1995). This polyphasic rise reflects the photoinduced reduction of the PSII electron carriers and transition of the reaction centres into a closed state (Govindjee, 1995). The two intermediate steps – *J* (2 ms) and –*I* (30 ms) reflect the transient accumulation of the reduced form of the primary quinone acceptor of PSII – Q_A (Strasser et al. 1995).

The fluorescence transient depends not just on the kinetic of the reactions that occurred on the donor and on the acceptor side of PSII quinone acceptors, but also on other factors as the chlorophyll content of the sample, the intensity of the actinic light, the temperature of the measurement. For this reason it cannot be used for direct comparison of the electron transport in PSII between the different samples. This can be done using the curves of the relative

variable fluorescence (V_t), that are calculated as ($V(t)=(F_t-F_o)/(F_m-F_o)$). Such representation reveals only the dynamic accumulation of Q_A^- ignoring any absorbance or heat dissipation differences. The changes in the shape of the fluorescence transient (the time course of Q_A^- accumulation) during the flight and post-flight period were followed by the V_t curves.

The different response of the strains to the space environment is described by the relative variable fluorescence curves presented at Figure. 18. The flight environment caused accumulation of reduced forms of PSII electron acceptors in IL but not in the A251C or I163N mutants. In fact, the mutants V_t curves registered on the flown samples were lower or very similar to the corresponding ground control (see the time range of 0.001-0.1 s). The wild type cc125 showed an increase of the relative amount of Q_A^- in comparison with the corresponding ground control during flight and particularly after landing (Figure.18). These results suggest that in this strain the processes involved in the re-oxidation of Q_A^- (for example the PSII photochemical reaction) have been impeded by the space conditions. In fact, cc125 showed low ability to maintain the level of its PSII electron transport after the landing; after the landing its F_v/F_m ratio dropped by 40% from the initial value while the double mutant *npq2 lor1* (Niyogi KK et al., 1997), showed sTable PSII performance during and after flight. In contrast, space flight did not have any effect on the PSII electron transport efficiency of the double mutant *npq2 lor1*.

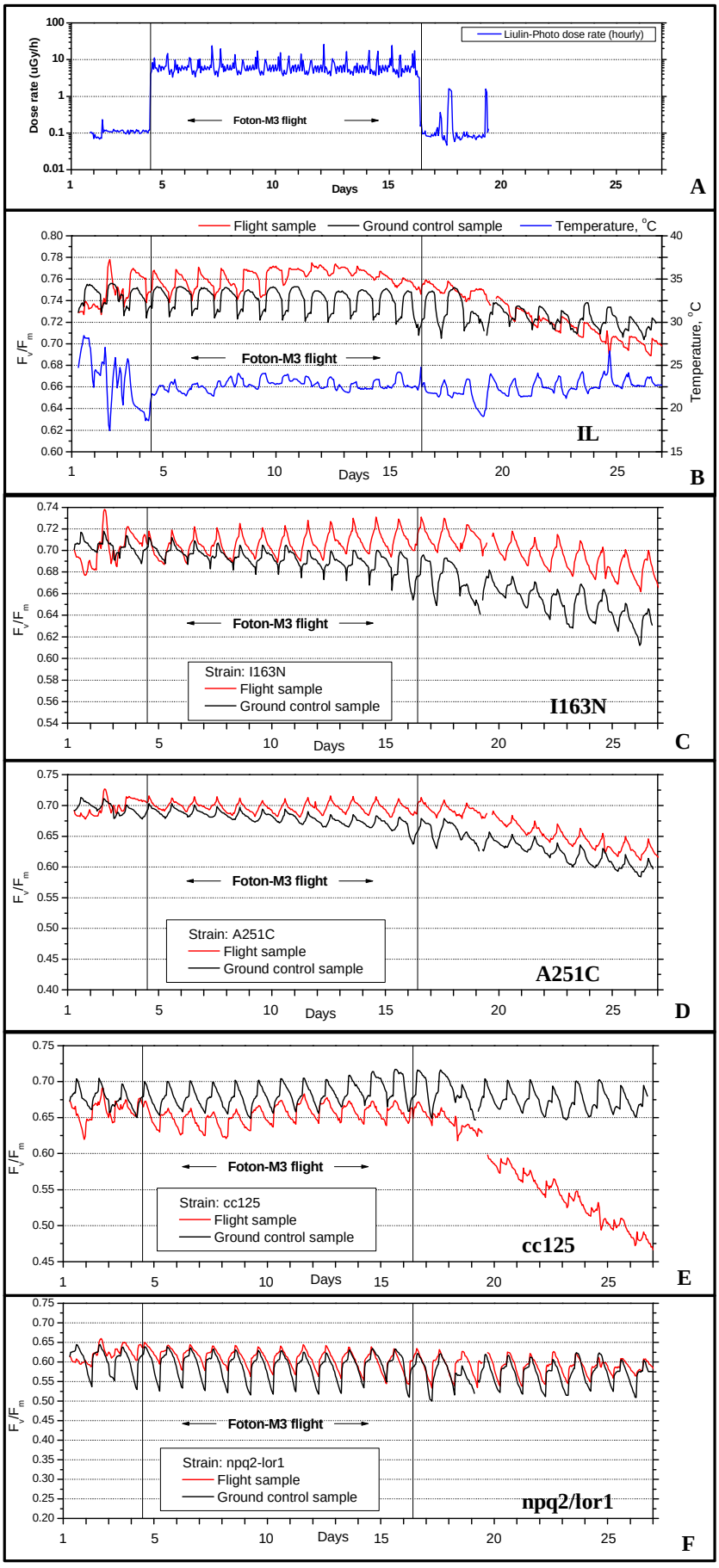

Figure 17 Real-Time Chl *a* fluorescence measurements recorded by the Photo II device during the Foton M3 mission. Fv/Fm values obtained by algal samples 5 days before, during the flight 12 days and 10 days after the flight. **Panel A**: Dose Ray adsorbed by the Liulin-Photo passive dosimeter; **Panel B**: on top, trend on the Fv/Fm values the parent strain IL; on bottom, profile of the Photo II recorded temperature (in blue); **Panel from C to F** trend on the Fv/Fm values in the analyzed strains, I163N, A251C, cc125, npq2lor1, respectively. Red and Black line correspond to flight and ground control sample, respectively.

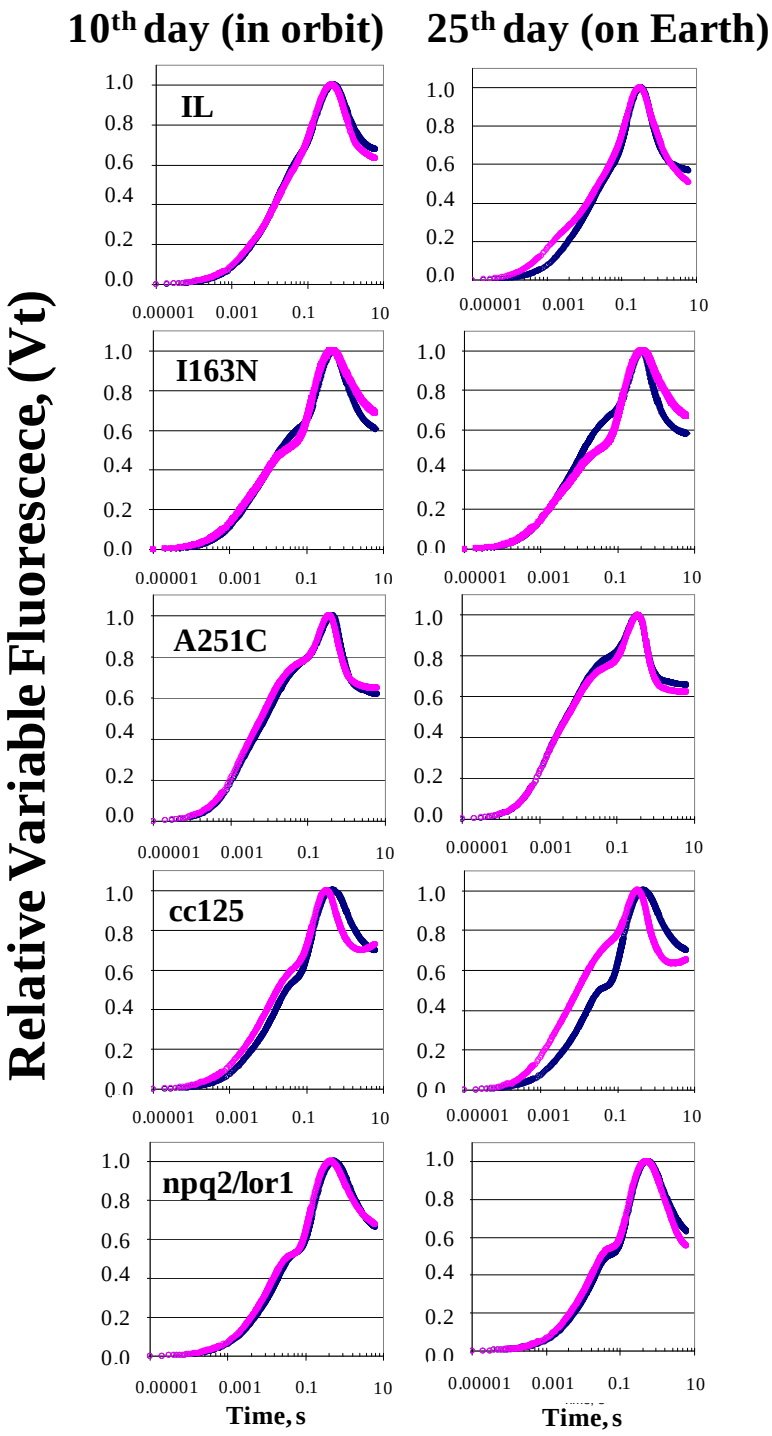

Figure 18 Fluorescence induction transient of *C. reinhardtii* mutants. Curves reported in the left and right panels refer to measurements carried out in flight (10^{th} day in orbit) and on Earth (25^{nd} day), respectively. The fluorescence curves recorded in the middle of the dark phase (after 8h dark), were used to calculate the relative variable fluorescence curves ($V_{(t)}$). Pink, in-flight samples; blue, on-ground controls.

4.1.2 Pigment content and composition

Quantitative analyses of carotenoids content and profile in the different exploited strains were carried out by HPLC in samples experienced the space environment and the corresponding samples grown on earth. As the mutants have different pigment accumulation levels compared to the parent strains even in physiological conditions, the content of pigments was expressed as a function of the Chl *a* content in order to normalised the data (Table 7).

PIGMENTS	STRAINS				
	IL	**I163N**	**A251C**	**cc125**	***npq2 lor1***
Violaxanthin					
Ground control	0.037	0.033	0.037	0.142	0.004
Flight	0.274	0.116	0.076	0.182	0.000
Zeaxanthin					
Ground control	0.031	0.014	0.021	0.058	2.118
Flight	0.091	0.051	0.047	0.059	3.538
Lutein					
Ground control	0.105	0.078	0.088	0.202	0.059
Flight	0.294	0.178	0.147	0.221	0.153
β-Caroten					
Ground control	0.985	0.403	0.624	3.178	7.671
Flight	1.066	2.274	1.532	0.677	1.423

Table 7. Pigment content in D1 mutant strains and NPQ mutants. Data are expressed as a mol:mol *ratio* compared to the Chl *a*. SE is between $2.4x10^{-4}$ and $1.0x10^{-6}$; n=6.

Carotenoids accumulation levels were modified in all the analysed D1 mutants with a similar regulation mechanism. Interestingly, in the I163N mutant violaxanthin and lutein displayed an approx. 3.5 and 2.2 fold increase respectively, while a 3.6 and 5.6 fold increase was detected for zeaxanthin and β-caroten. In the case of β-caroten, induction levels were higher in mutants compared to the parental strain IL. Similar results were also obtained for the A251C mutant, even if induction levels were lower compared to those detected in I163N. In IL parent strain, all the pigments increased with the exception of β-caroten, Concerning the NPQ set of strains, it is noticeable the 2.6 fold increase of lutein detected in the double NPQ-mutant *npq2 lor1* (impaired in xanthopyll cycle biosynthesis) and the 5.5 fold decrease of ß-caroten. Zeaxanthin levels were slightly increased reaching a 1.7 fold change. β-caroten levels decreases were also observed in the wild-type cc125 showing a 4.7 fold variation. In general

the NPQ strains have a higher basal levels of pigments compared to the D1 strains, so it is not surprising to observe a different accumulation pattern. a-caroten and chlorophyll levels did not show any significant changes (data not shown).

4.1.3 q RT-PCR expression profiling

To test if the expression levels of genes involved in the biosynthesis of carotenoids, plastoquinones and PSII-D1 and D2 proteins are transcriptionally influenced by space radiation, we set up a quantitative real-time polymerase chain reaction (q-RT PCR) protocol. Analyses were carried out on RNA extracted by algal samples 3 days after landing. Expression analyses on *psbA* gene encoding the D1 protein, revealed an approx. 3 fold increase in IL and I163N and at least 2-fold increase in the most analyzed strains (Figure 19). An exception is represented by the wild type cc125 strain, in which the *psbA* transcript accumulation level was not significantly affected. Concerning the *psbD* gene, encoding the D2 protein, no important changes in the transcript accumulation levels were observed in any of the analyzed strains. Regarding the expression levels of genes involved in plastoquinone pathway (*hst1*, *mpbq-mt*) we found different behaviors through the strains (Figure 19). In particular, accumulation levels of plastoquinone encoding genes, displayed a strong down regulations in all the D1 and *npq2 lor1* mutants; in the wild-type cc125 no changes were observed while in IL the control reference strain, a 2-fold increased was induced.

Interestingly, concerning the expression levels of gene involved in the carotenoids biosynthetic pathway, a general repression was observed, in particular in those genes encoding enzymes involved in the biosynthesis of zeaxanthin and β-caroten, as *vdr* and *lyc*β respectively. *Vdr* gene was down-regulated in all the analyzed strains, reaching the highest value in the double mutant *npq2 lor1* reporting a 11.2 fold change decrease. *Lyc*β was down regulated only in the D1 set, particularly in IL. Beside a strong up regulation of 8.6 fold change was observed in cc125 but not in the *npq2 lor1* mutant that was unaffected. Also *pds*, that catalyzed the desaturation of phytoene, was down regulated, reaching approx. 4 fold change down-regulation. An opposite trend was observed only for *psy* gene expression that was up regulated in all the D1 set, reaching the highest value of 58 fold change increase in A251C mutant, while negligible differences were observed in the NPQ set (Figure 19).

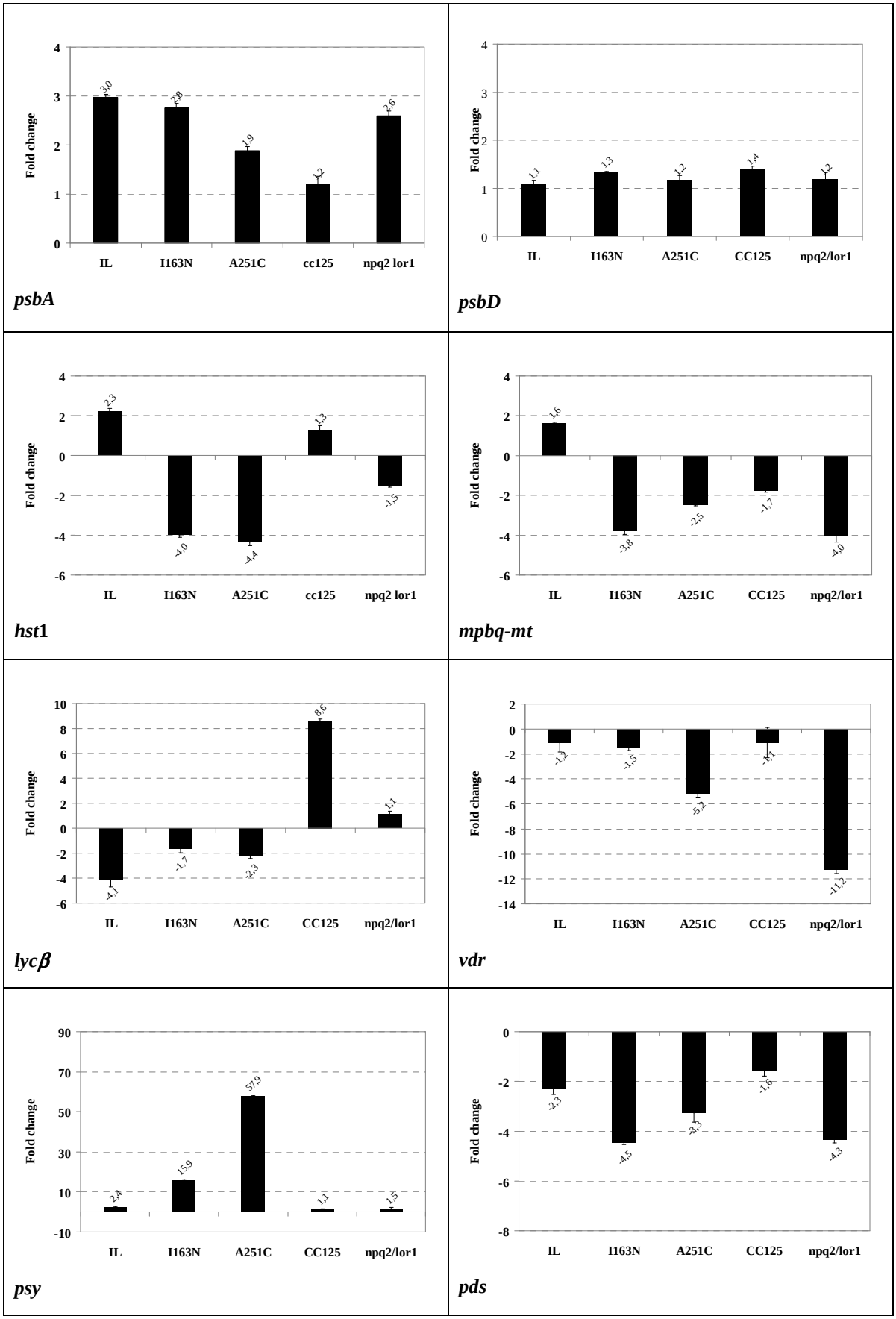

Figure. 19. Gene expression level of *C. reinhardtii* in strains that experienced the Space radiation environment during the Foton M3 Space mission.

4.2 STS-134 Space Mission Results

In a previous study, *in vitro* directed evolution strategies targeted at the D1 protein were adopted to create a library of *Chlamydomonas* random mutants, subsequently selected by exposures to radical-generating proton or neutron sources (Rea et al., 2011). A first set of these mutants were produced also by site-directed mutagenesis and included in the Foton M3 experiment previously described.

In this thesis, a second set of the previously identified aminoacidic substitutions, close to the secondary plastoquinone binding niche and the oxygen evolving complex, were introduced by site-directed mutagenesis in un-transformed strains, and their sensitivity to free radicals attack analyzed. The characterization of these strains allowed to determine the mutants suiTable to be used as life regenerative supporting system in long-term space missions and were included in the PHOTOEVOLUTION experiment flown aboard the STS-134 mission.

4.2.1 Production and characterization of *Chlamydomonas* D1 site-directed mutants

The *in vitro* evolution experiment led to the isolation of random mutants tolerant to neutron and proton exposure revealing that single aminoacidic substitution in the D1 protein could contribute to ionizing radiation tolerance. To exclude the possibility that additional random mutations induced by the radiation exposure could confer the observed tolerance, a set of the identified amino acid substitutions were introduced by site-directed mutagenesis in untransformed strains. The choice of the aminoacidic substitutions was made to include mutations located in two different structural regions of the D1 protein, near Tyr161 and the OEC (I163T, P162S, M172L) and near the Q_B binding pocket (G207S, L200I, I281T)

Physiological characterization of the obtained mutants was carried out by estimating the growth parameters and the photosynthetic efficiency. The mixotrophic growth rate was followed for a period of four days, revealing very similar trends among the different mutants and compared to the control reference strain IL (Figure. 20). In contrast, the mutants and the control strain showed differences in their chlorophyll content (Figure. 20) and photosynthetic performance.

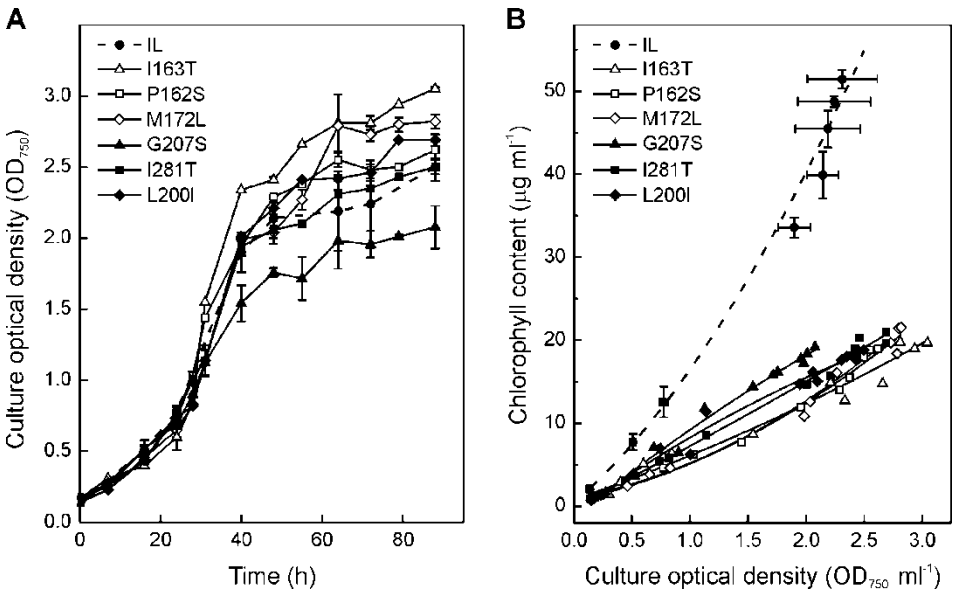

Figure. 20 Physiological characterizations of *C. rheinardtii* mutants in terms of mixotrofic growth rate (A) and Chlorophyll content (B)

The mutants generally showed a lower maximal quantum yield of PSII photochemistry (F_v/F_m) and a reduced efficiency of the electron transport through PSII primary and secondary electron acceptors (1- V_J) than the control strain (Figure. 21). These findings clearly indicate a reduction in the efficiency of the light energy utilization in the mutant strains compared to control in physiological conditions. Thus, these statistically significant differences indicate the relevance of a single amino acid substitution in D1 for the function of PSII, in agreement with previous results. The extent of the reduction in the fluorescence parameters was not strictly related to the position of the amino acid substitution, as a general reduction of PSII performance was observed in both groups of mutants (Figure. 21).

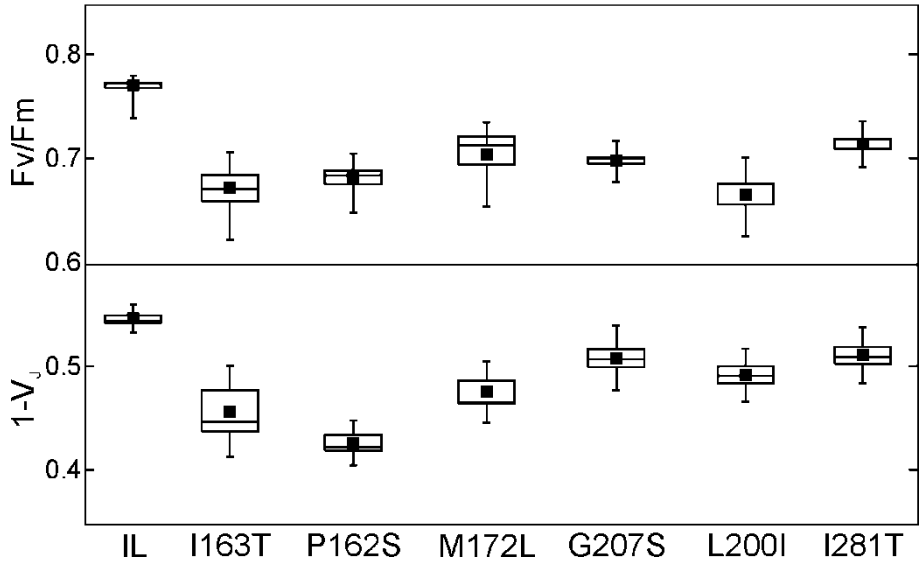

Figure 21. Maximum quantum yield and electron transport efficiency of the site-directed *Chlamydomonas* D1 mutants. Fluorescence parameters of the reference strain, IL, and the D1 site-directed mutants of *C. reinhardtii* were calculated from the fluorescence induction curve. The statistical distributions for the maximum quantum yield of PSII photochemistry, Fv/Fm = (Fm-Fo)/Fm, and the efficiency of the electron transport between the primary (Q_A) and secondary (Q_B) PSII electron acceptors , $1\text{-}V_J = 1 - (F_{2ms}\text{-}F_o)/(Fm\text{-}F_o)$, are presented as box and whiskers plots. The measurements were performed on liquid cell cultures containing equal amounts of chlorophyll (14±1 µg ml^{-1}) after 10 min of dark adaptation. The statistical analysis was performed on average values, obtained from at least four experiments, n=9-20. The mutants resulted statistically different from the reference strain at P=0.05.

Despite the lower electron transfer efficiency, a higher oxygen evolution capacity under high photon fluency conditions was demonstrated in all the mutants compared to the reference strain, IL (Figure. 22). The rate of O_2 production of the mutants and the control strain were very similar under 200 µmol·m^{-2} s^{-1} light intensity, which was already saturating for the photosynthetic reactions of IL strain. On the contrary, D1 mutants were able to achieve and maintain more than two-fold higher O_2 evolution rate even under the very high light intensity of 900 µmol·m^{-2} s^{-1}.

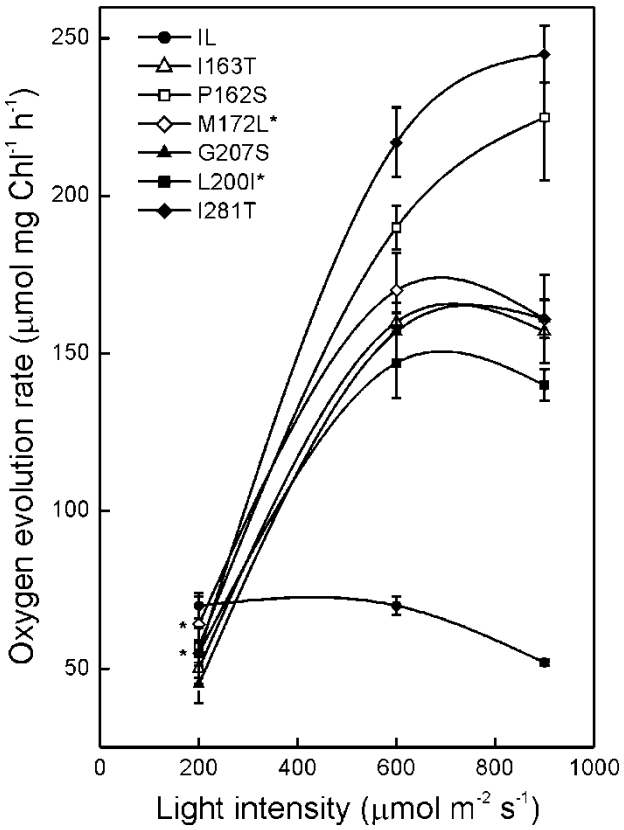

Figure 22. Light-dependent oxygen evolution capacity of the site-directed C*hlamydomonas* D1 mutants. The curves were recorded by gradual increase of the light intensity from 200 up to 900 µmol m^{-2} s^{-1}. Measurements were performed on liquid cell cultures containing equal amounts of chlorophyll (15±2 µg ml^{-1}), in the presence of 10 mM $NaHCO_3$ as additional carbon source. Values are the average of three independent experiments, ±SE, n=9. The mutants resulted statistically different from the reference strain at P=0.05, except the cases M172L and L200I at 200 µmol m^{-2} s^{-1} indicated by an asterisk.

4.2.2 Photosynthetic efficiency of site-directed mutants

Light intensity is a vital factor in photosynthetic organisms. However excessive doses can severely damage the photosynthetic apparatus due to production of high levels of free radicals. To test the capability of the selected mutants to cope with the challenge of the high irradiance conditions, we monitored changes in their PSII efficiency in the presence of stressful high light intensity by real-time measurements of the F_v/F_m ratio. In the reference strain IL under control light conditions, the changes of the F_v/F_m values as a result of two contiguous exposures to light and darkness were negligible (Figure. 23). On the contrary, under high irradiance, the PSII performance tended to decrease with the onset of the light, showing the pattern of accumulation of the photo-induced oxidative pressure. However, the reduction was reversible, since during the following dark phase a recovery of the maximum quantum yield of PSII photochemical reaction occurred (Figure. 23). We have to point out that the light intensity that the *Chlamydomonas* strains could support depends strongly on the

growth illumination and the physical phase of the nutrition medium. According to our experiments and in confirmation to the data presented in (Figure. 23)., when the algal cells are immobilized on a solid medium a light intensity as low as 150 µmol·m^{-2} s^{-1} could induce photoinhibitory PSII damage. The injury could be permanent, leading to the cell death, or reversible, depending on the stress duration.

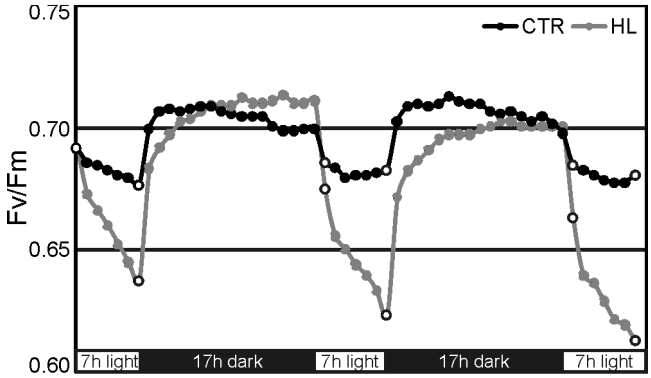

Figure 23. Daily trend of PSII photochemistry during two consecutive light/dark cycles in the reference strain IL. Cell cultures containing equal amounts of chlorophyll were immobilized on TAP agar medium and the Fv/Fm ratio was measured hourly in both growth (50 µmol m^{-2} s^{-1}, CTR, black line) and high light conditions (150 µmol m^{-2} s^{-1}, HL, grey line). Photoinhibition is evident by the reduction of the Fv/Fm recorded during the light phases under HL compared to CTR photon fluency. The open circles indicate the first and the last point of the light phase. The reported curves are representative of three independent experiments, n=6. SE < 3%.

All the analyzed strains displayed a high capacity to tolerate the applied stress. In fact, over the monitored period, decrease of photosynthesis efficiency ranged from 1 to 13% (Figure. 24). The maximum reduction level was observed in the reference strain IL (13%), that showed the worst performance compared to the mutants. In this strain, in fact, after only two days of treatment, the maximum quantum yield dropped by 6%, and continuously declined during the subsequent days. Concerning the mutants, no correlation was observed between amino acid localization and photosynthetic activity. However, different mutants behaved in a different manner: I163T, L200I and I281T maintained very sTable photosynthetic efficiency, reporting maximum 3.4% reduction of Fv/Fm values; G207S and P162S were less sTable, gradually losing about 7% of the initial activity. M172L provided results similar to IL, displaying a photosynthetic reduction of about 10%.

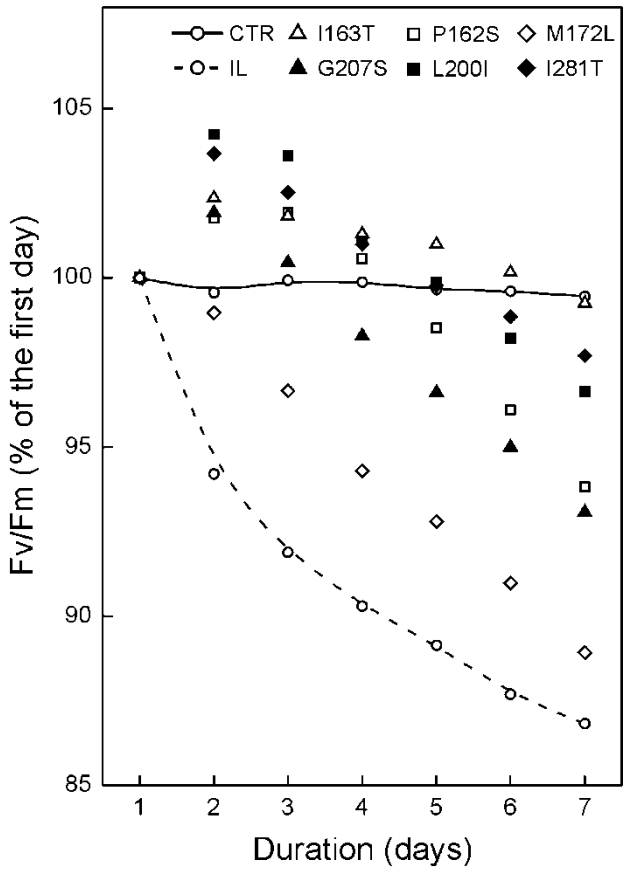

Figure 24. Time-course of PSII photochemistry at high photon fluency in the site-directed *Chlamydomonas* D1 mutants. Cell cultures containing equal amounts of chlorophyll (80 µg) were immobilized on TAP agar medium and the Fv/Fm ratio was measured hourly in both growth (50 µmol m^{-2} s^{-1}) and high light conditions (150 µmol m^{-2} s^{-1}). The reported values are measured at the onset of each light phase and are reported as percentage of the Fv/Fm ratio calculated with respect to the first day. All the analysed strains displayed a good capacity to tolerate the applied photoinhibitory light intensities (150 µmol m^{-2} s^{-1}). The maximal photosynthetic efficiency reduction was observed in the reference strain IL compared to the produced site-directed mutants. The control line (CTR) corresponds to an average value of all characterised strains and was obtained from samples exposed to 50 µmol m^{-2} s^{-1}. The reported values are the average of three independent experiments; for the sake of clarity bars of standard errors are omitted, the maximum SE being < 3%. The mutants resulted statistically different from the reference strain at P=0.05.

4.2.3 The PHOTOEVOLUTION Project

The achievement of site-directed mutants with improved oxygen evolution capability in stressful conditions, prompted us to exploit these organisms in the PHOTOEVOLUTION Project.

Before flight, the experimental set-up was optimised in order to get vital cells in space. Selected mutants (IL, I163T, I163N, P162S) were tested on ground for their capability to tolerate the immobilization conditions on solid medium inside the PHOTO I device, modulating cells concentration and medium content (volume). Viability was tested in the presence or absence of light, in order to determine the minimal and maximum duration times without loss of life. Among the different possibilities, we choose the best allowing the strains survival for about one months without significant physiological changes. These conditions are reported in material and methods.

The photosynthetic performance of the site-directed mutants was determined by chlorophyll fluorescence analyses using the Fluorescence Monitoring System (FMSII, Hansatech, King's Lynn, Norfolk, UK). Photosynthetic performance was monitored to reveal health status of the algae. Fluorescence measurements were performed analyzing all the strains at different time during the entire duration of the experiment: i - arrival at the Kennedy Space Centre (just before the flight), ii - After the retrieval and storage of the samples (before to leave the NASA complex), iii - at the arrival to the principal investigator laboratory.

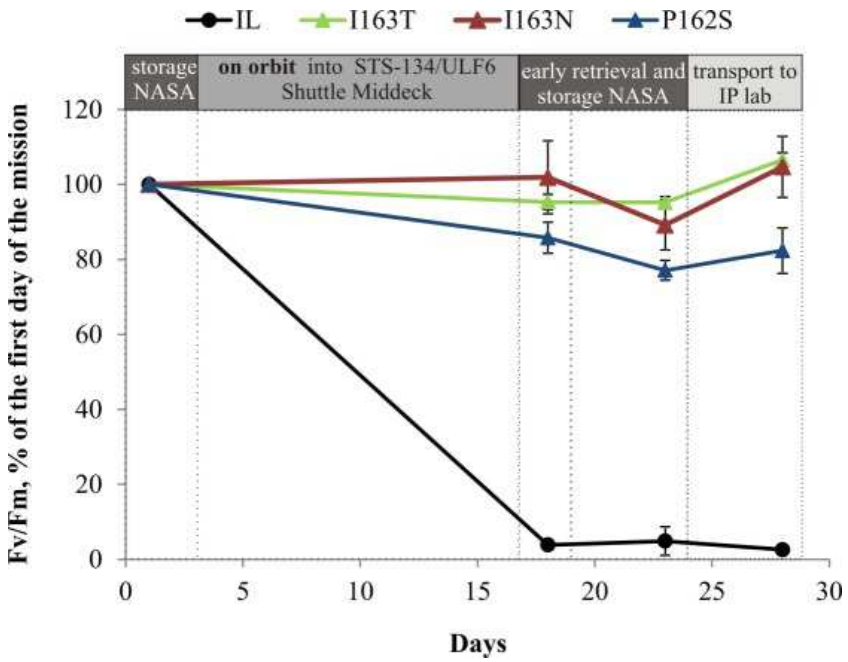

Figure 25. PSII fluorescence monitoring of strains experienced the space environment during the STS-134 mission.

In Figure 25, the photosynthetic performance of the analyzed strains is shown, reported as percentage values relative to the first day of measurement. It is immediately clear that all the D1 mutants were capable to perform photosynthesis maintaining sTable Fv/Fm ratio. In particular, fluorescence parameters recorded in I163N and P162S mutants revealed a slight decrease of approx. 13 and 19 % on the last analyzed day (29th day). Surprisingly, the I163T mutants show a 6% fluorescence increase compared to the first day of measurement. Despite the mutant's photosynthetic performance stability, the D1 parent strain, IL, was dramatically affected by the ISS environment showing a strong fluorescence decrease of 70%.

5 - DISCUSSION

In the near past, human life in Space was a quite impossible task to achieve. Nowadays people can survive and work for long time in space aboard of the ISS. However, long-term space mission sustaining requires to bring new food stocks and restore atmospheric condition (new oxygen). The maintenance of a healthy status, limited food sources together with the presence of microgravity and radiation environment are the main problems that need to be solved in order to permit human life in space.

Photosynthetic organisms provide food and oxygen through photosynthesis on earth and as a consequence they should be present also in space. They can use the carbon dioxide emitted by the astronauts producing new oxygen and at the same time they could be used as food supplementation, but the presence of ionizing radiation can damage all kind of life that we know so far.

For this reason, it is important to find good candidates able to tolerate this harsh environment.

We tested the capacity of photosynthetic microalgae to cope with the space environment exploiting *C. reinhardtii* wild type, NPQ-mutants (*npq2 lor1*) and D1- radiation (I163N) and herbicide (A251C) tolerant mutants during the space mission Foton M3 (2007). Chlorophyll fluorescence measurement was used as health indicator parameter as it is directly connected to the PSII electron flow efficiency, which is among the main target of radiation-induced damage. During this mission in the lower terrestrial orbit, the dose rate measured by the active spectrum-dosimeters Liulin-Photo was approx. 10 μGy/h (Damasso et al., 2009), a value 100 times higher compared to that received on earth.

To understand the real space effects on *C. reinhartii* strains each mutant was compared to the corresponding ground control. Fluorescence measurements recorded during the flight showed that all the analyzed strains were able to maintain their photosynthetic maximum quantum yield loosing at least a 10% of the initial performance (IL, I163N, A251C, cc125, *npq2 lor1*). Among these strains, only the I163N, A251C and the double *npq2 lor1* mutants maintained active photosynthetic electron transport rate after landing (Figure. 17, 18). In particular, the I163N strain was selected under neutrons exposure and confirmed its space radiation tolerance maintaining approx. 99% of its initial fluorescence value. Probably, the aminoacid substitution, close to the Q_B binding pocket and oxygen evolution site, in A251C and I163N mutant strains plays an important role to overcome the oxidative radiation damages. Similarly, the double mutant *npq2 lor1* was able to efficiently counteract the extreme space environment, while the corresponding wild-type cc125 was less efficient. The ability to

accumulate zeaxanthin, a well known radical scavenger molecule, probably helps this strain to avoid oxidative damages. The *npq2 lor1* mutant resistance strongly suggests an involvement of antioxidant pigments accumulation in the tolerance against radiation exposure.

On return on earth, we performed transcript analyses revealing a general up regulation of the *psbA* gene in all the analyzed strains. It is possible to hypothesize that, similarly to high-light acclimation responses (Depka et al., 1998), space environment damages the D1 and PSII core complex determining an induced rate of the D1 protein turn-over most probably affecting also the transcript level of the *psbA* gene.

The general increase of antioxidant pigment accumulation levels was not correlated to the steady state accumulation of genes involved in their biosynthesis. In particular, to the strong repression observed in *zep* and *vdr* gene expression levels corresponded an increased accumulation of zeaxanthin observed in mutants having enhanced photosynthetic stability. In this context, it has been hypothesized the activation of a feedback regulation mechanism induced by the end-product, in agreement to what has been observed also by Herrin et al., 1992. The only exception is represented by the psy gene which operating up-stream of the pathway in the biosynthesis of phytoene is most probably out of the control operated by an end-product.

Regarding plastoquinone biosynthesis, it has been recognized that in higher plants oxidized quinones have an induction role in phytoene desaturase activity leading to the activation of the carotenoids biosynthetic pathway. On the contrary, reduced quinones were ineffective (Mayer MP et al., 1990). In particular, plastoquinone biosynthesis resulted generally repressed in mutants capable to counteract the space environment, but not in the reference strains. This phenomenon could represent the successful key for their enhanced stability. Fluorescence data point out that space conditions interfere with plastoquinone pool redox state (Figure.18), resulting in a lower expression level of genes involved in this biosynthetic pathway. In the D1 mutants, the high D1 protein turnover and the mutation in the Q_B pocket could prevent the plastoquinone over-reduction, that on the contrary is over-reduced in the parent IL strain. Similarly, in the wild-type cc125 the re-oxidation photochemistry was reduced contrary to what observed in the double mutant *npq2 lor1*. This phenomenon suggested a major availability of oxidized plastoquinone in the plastoquinone pool that could account for a highest desaturation of phytoene as observed in Mayer and co-workers (1990). The rate of plastoquinone biosynthesis it is probably modulated through the plastoquinone pool redox state that indirectly influence the carotenoids biosynthetic pathway with availability of the substrate geranylgeranyl-diphospate and the oxidized quinones that catalyze the desaturation of phytoene.

Regarding carotenoids accumulation, it was observed that in high light condition zeaxanthin is the most accumulated pigment, acting as radical scavenger. Beside also beta-caroten and lutein play a fundamental role as radical scavenger during high light stress pressure. In this work, we demonstrated how strains which accumulate high content of antioxidant compounds (beta-caroten, zeaxanthin) are more sTable in real space conditions.

The observed pigments accumulation was different in all the analyzed strains, even if a common trend was observed for beta-caroten the most accumulated in all the D1 mutants reaching the highest value in I163N and A251C strains. Instead, beta-caroten and zeaxanthin were the most accumulated pigments in the double mutant *npq2 lor1*.

Similar results were obtained over-expressing *psy* gene in *Arabidopsis thaliana* plants (Lindgren LO et al., 2003) showing a strong increase of beta-caroten. Probably the accumulated pigment act as radical scavenger as observed during high light exposure.

Pigments accumulations together with psy over expression are in agreement with the previous observed results and the generally repressed plastoquinone biosynthetic pathway suggesting that more substrate is available for carotenoids biosynthetic pathway. The highest photosynthetic stability was observed in the I163N, A251C and *npq2 lor1* double mutant in which the beta-caroten and zeaxanthin accumulation were the highest.

The possibility to join to a second Space mission (Endeavour STS-134, 2001), was fundamental to further investigate basic mechanisms of space radiation tolerance.

To achieve this goal it was essential the selection on ground of the best performing strains to stressful conditions. The production of site-directed mutants allowed to exclude the presence of casual gene modifications possibly induced by the radiation exposures adopted in the in vitro evolution experiments.

The measurements recorded under the applied stressful conditions revealed an increased photosynthetic performance stability and oxygen evolution capacity (Figure. 19; Figure. 20). It was demonstrated how the generation of reactive oxygen species under high light condition can induce oxidative stress (Hideg E et al., 2000; Nishiyama Y et al., 2006).

In particular, the interaction between free electrons with oxygen molecules, tyrosine residues and chlorophylls leads to the formation of dangerous radical species as singlet oxygen, hydrogen peroxide, hydroxyl radical, Tyr radical and chlorophyll triplets that can compromise the PSII functionality (Edelman M, and Mattoo AK, 2008; Ledford HK, and Niyogi KK., 2005; Zeng XQ et al., 2010). Thus, our experimental results demonstrate that the D1 amino acid substitutions responsible for the high light exposure resistance, could also account for the improved radiation tolerance of the site directed mutants (Rea et al., 2011).

The data presented in this thesis clearly indicated that space tolerance has multi-factorial component including the synthesis of antioxidant pigments, an increased oxygen evolution capacity and the localization of the mutations regarding the D1 strains. We demonstrated that even single amino acid substitutions in D1 protein enable the cells to survive in the presence of free radicals produced by both high light fluency and ionizing radiation.

Beside this approach allows the selection of mutants with improved stability, a parameter of great interest in any biotechnological application of photosynthetic proteins spanning from space research to biosensors and photovoltaic fields, including biofuel and nutraceuticals production [44].

6 – REFERENCES

Alpen E. (1990). *Radiation Biophysics*. 2° ed., edn. Academic Press, San Diego, California.

Ambesi Impiombato FS, Curcio F, Meli A, Zambito AM. (2006). Fresh new air in space? 'MoMa' on the A.S.I. launch pad. *Orig Life Evol Biosph.*; **36(5-6)**: 577-85.

Anwaruzzaman M, Chin BL, Li X-P, Lohr M, MartinezDA and Niyogi KK. (2004). Genomic analysis of mutants affecting xanthophyll biosynthesis and regulation of photosynthetic light harvesting in *Chlamydomonas reinhardtii*. *Photosynthesis Research;* **82(3)**: 265:276.

Asada K. (1996). Radical production and scavenging in the chloroplasts. In: Baker NR (ed) Photosynthesis and the environment. *Kluwer Academic Publishers, Dordrecht, The Netherlands*, pp.123–150.

Asada K. (1999). THE WATER-WATER CYCLE IN CHLOROPLASTS: Scavenging of Active Oxygens and Dissipation of Excess Photons. *Annu Rev Plant Physiol Plant Mol Biol.*; **50**: 601-639.

Baroli I, Do AD, Yamane T, Niyogi KK. (2003). Zeaxanthin accumulation in the absence of a functional xanthophyll cycle protects *Chlamydomonas reinhardtii* from photooxidative stress. *Plant Cell;* **15**: 992–1008.

Barros T, and Kühlbrandt W. (2009). Crystallisation, structure and function of plant

Beauregard G, Potier M. (1985). Temperature Dependence Of The Radiation Inactivation Of Proteins. *Analitical Biochemistry;* 150: 117-120.

Biesalski HK, and Obermueller-Jevic UC. (2001). UV light, beta-carotene and human skin--beneficial and potentially harmful effects. *Arch Biochem Biophys*; **389(1)**:1-6.

Billi D, Friedmann EI, Hofer GK, Grilli Caiola M, and Ocampo-Friedmann R. (2000). Ionizing-Radiation Resistance in the Desiccation-Tolerant Cyanobacterium Chroococcidiopsis. *Appl. Environ. Microbiol;* **66:** 1489-1492.

Bohne F and Linden H. (2002). Regulation of carotenoid biosynthesis genes in response to light in *Chlamydomonas reinhardtii*. *Biochimica and Biophysica Acta;* **1579**: 26–34.

Bonk M, Hoffmann B, Von Lintig J, Schledz M, Al-Babili S, et al. (1997). Chloroplast import of four carotenoids biosynthetic enzymes in vitro reveals differential fates prior to membrane binding and oligomeric assembly. *European Journal of Biochemistry;* **247**: 942–50.

Boussiba S. (2000). Carotenogenesis in the green alga *Haematococcus pluvialis*: cellular physiology and stress response. *Physiol. Plant;* **108:**111–17.

Bouvier F, d'Harlingue A, Hugueney P, Marin E, Marion-Poll A, and Camara B. (1996). Xanthophyll biosynthesis. Cloning, expression, functional reconstitution, and regulation of beta-cyclohexenyl carotenoid epoxidase from pepper (*Capsicum annuum*). *The Journal of Biological Chemistry;* **271**: 28861–67.

Bouvier F, Keller Y, d'Harlingue A, and Camara B. (1998). Xanthophyll biosynthesis: molecular and functional characterization of carotenoid hydroxylases from pepper fruits (*Capsicum annuum* L.). *Biochimica et Biophysica Acta;* **1391**: 320–28.

Britton G. (1998). Overview of carotenoid biosynthesis. Britton G, Liaaen-Jensen S, Pfander H, eds. 1998. *Carotenoids: Biosynthesis and Metabolism*. Basel: Birkhäuser, pp. 13–147

Bugos RC, and Yamamoto HY. (1996). Molecular cloning of violaxanthin de-epoxidase from romaine lettuce and expression in *Escherichia coli*. *Proceedings of the National Academy of Sciences of the United States of America;* **93**: 6320–25.

Bugos RC, Hieber AD, and Yamamoto HY. (1998). Xanthophyll cycle enzymes are members of the lipocalin family, the first identified from plants. *The Journal of Biological Chemistry;* **273**: 15321–24.

Caffarri S, Croce R, Breton J, and Bassi R. (2001). The major antenna complex of Photosystem II has a xanthophyll binding site not involved in light harvesting. *J Biol Chem* **276**: 35924–35933.

Cano JB, Giannini D, Pezzotti G, Rea G, and Giardi MT. (2011). Space Impact and Technological Transfer of a Biosensor Facility to Earth Application for Environmental Monitoring. *Recent Patents on Space Technology;* **1:** 000-000 1.

Carol P and Kuntz M. (2001). A plastid terminal oxidase comes to light: implications for carotenoid biosynthesis and chlororespiration. *Trends in Plant Science;* **6**: 31–36.

Chunayev AS, Mlrnaya ON, Maslov VG, and Boschetti A. (1991). Chlorophyll b and chloroxanthin-deficient mutants of *Chlamydomonas reinhardtii*. *Photosynthetica* **25:** 291-301.

Cogdell RJ. (2006). The structural basis of non-photochemical quenching is revealed? *Trends Plant Sci.*; **11(2)**: 59-60.

Coggle JE. (1998). Effetti biologici delle radiazioni, 3° ed edn. Edizioni Minerva Medica, Torino, Italy.

Cunningham FX Jr, and Gantt E. (1998). Genes and enzymes of carotenoid biosynthesis in plants. *Annual Review of Plant Physiology and Plant Molecular Biology;* **49**: 557–83.

Cunningham FX Jr, and Gantt E. (2001). One ring or two? Determination of ring number in carotenoids by lycopene epsiloncyclases. *Proceedings of the National Academy of Sciences of the United States of America;* **98**: 2905–10.

Cunningham FX Jr, Pogson B, Sun Z, McDonald KA, DellaPenna D, Gantt E. (1996). Functional analysis of the β and ε lycopene cyclase enzymes of Arabidopsis reveals a mechanism for control of cyclic carotenoid formation. *Plant Cell;* **8**: 1613–1626.

Dall'Osto L, Cazzaniga S, Havaux M, and Bassi R. (2010). Enhanced photoprotection by protein-bound vs free xanthophyll pools: A comparative analysis of chlorophyll b and xanthophyll biosynthesis mutants. *Mol. Plant*.; **3**: 576–593.

Dall'Osto L, Fiore A, Cazzaniga S, Giuliano G, and Bassi R. (2007). Different roles of alpha- and beta-branch xanthophylls in photosystem assembly and photoprotection. *J Biol Chem.*; **282(48)**: 35056-68.

Damasso M, Dachev T, Falzetta G, Giardi MT, Rea G, et al. (2009). The radiation environment observed by Liulin-Photo and R3D-B3 spectrumdosimeters inside and outside Foton-M3 spacecraft. *Radiat Meas*, **44**: 263–272.

Danon A, and Mayfield SP. (1991). Light-regulated translational activators: identification of chloroplast gene specific mRNA binding proteins. *EMBO J*., **10**: 3993–4001.

Dauvillee D, Hilbig L, Preiss S, et al. (2004). Minimal extent of sequence homology required for homologous recombination at the *psbA* locus in *Chlamydomonas reinhardtii* chloroplasts using PCR-generated DNA fragments. *Photosynth Res;* **79:** 219-224.

Davies JP, Yildiz FH, and Grossman A. (1996). Sac1, a putative regulator that is critical for survival of *Chlamydomonas reinhardtii* during sulfur deprivation. *EMBO J*, **15**: 2150–2159.

Davies JP, Yildiz FH, and Grossman AR. (1994). Mutants of Chlamydomonas with aberrant responses to sulfur deprivation. *Plant Cell,* **6**: 53-63.

Debuchy R, Purton S, Rochaix JD. (1989). The argininosuccinate lyase gene of *Chlamydomonas reinhardtii*: an important tool for nuclear transformation and for correlating the genetic and molecular maps of the *ARG7* locus. *The EMBO journal*; **8**: 2803-2809.

Depka B, Jahns P, and Trebst A. (1998). Beta-carotene to zeaxanthin conversion in the rapid turnover of the D1 protein of photosystem II. *FEBS Lett*.; **424(3)**: 267-70.

Derguini F, Mazur P, Nakanishi K, Starace DM, Saranak J, and Foster KW. (1991). All-trans-retinal is the chromophore bound to the photoreceptor of the alga *Chlamydomonas reinhardtii*. *Photochemistry and Photobiology*; **54**: 1017–21.

Edelman M, and Mattoo AK. (2008). D1-protein dynamics in photosystem II: the lingering enigma. *Photosynth Res* **98**: 609–620.

Ellstrand NC. (2001). When transgenes wander, should we worry? *Plant Physiol*; **125**: 1543-5.

Ellstrand NC. (2003). Current knowledge of gene flow in plants: implications for transgene flow. *Philosophical transactions of the Royal Society of London. Series B, Biological sciences*; **358**: 1163-70.

Emanuelsson A, Eskling M, and Akerlund HE. (2003). Chemical and mutational modification of histidines in violaxanthin de-epoxidase from *Spinacia oleracea*. *Physiologia Plantarum;* **119**: 97–104.

Erickson JM, Rahire M, and Rochaix JD. (1984). *Chlamydomonas reinhardtii* gene for 'the 32000 mol. wt. protein of photosystem II contains four large introns and is located entirely within the chloroplast inverted repeat. *EMB0 J*., **3:** 2753-2762.

Ferris PJ. (1995). Localization of the nic-7, ac-29 and thi-10 genes within the mating-type locus of *Chlamydomonas reinhardtii*. *Genetics*; **141**: 543-549.

Formaggio E, Cinque G, and Bassi R. (2001). Functional architecture of the major light-harvesting complex from higher plants. *Journal of Molecular. Biology;* **314:** 1157–1166.

Fraser PD, Romer S, Shipton CA, Mills PB, Kiano JW, et al. (2002). Evaluation of transgenic tomato plants expressing an additional phytoene synthase in a fruit specific manner. *Proceedings of the National Academy of Sciences of the United States of America;* **99**: 1092–97.

Fray RG, Wallace A, Fraser PD, Valero D, Hedden P, et al. (1995). Constitutive expression of a fruit phytoene synthase gene in transgenic tomatoes causes dwarfism by redirecting metabolites from the gibberellin pathway. *The Plant Journal;* **8**: 693–701.

Galbinur T, Obolensky A, Berenshtein E, Vinokur V, Chowers I, Chevion M, Banin E. (2009). Effect of para-aminobenzoic acid on the course of retinal degeneration in the rd10 mouse. *J Ocul Pharmacol Ther.*; **25(6)**: 475-82.

Gastaldelli M, Canino G, Croce R, and Bassi R. (2003). Xanthophyll binding sited of the CP29 (Lhcb4) subunit of higher plant Photosystem II by domain swapping and mutant analysis. *J Biol Chem* **278**: 19190–19198.

Goodenough UW. (1992) Green yeast. *Cell*; **70(4):**533-8.

Govindjee. (1995). Sixty-three years since Kautsky: Chlorophyll a Fluorescence. *Aust . Plant Physiol*.; **22**: 131-160.

Grossman AR, Croft M, Gladyshev VN, Merchant SS, Posewitz MC, Prochnik S, and Spalding MH. (2007). Novel metabolism in *Chlamydomonas* through the lens of genomics. *Curr Opin Plant Biol*; **10(2):** 190-198.

Grossman AR, Harris EE, Hauser C, Lefebvre PA, Martinez D, Rokhsar D, Shrager J. (2003). *Chlamydomonas reinhardtii* at the crossroads of genomics. *Eukaryot Cell.;* **2(6):**1137-50.

Grossman AR, Lohr M, and Im CS. (2004). *C. reinhardtii* in the landscape of pigments. *Annu Rev Genet.*; **38**: 119-73.

Gumpel NJ, Ralley L, Girard-Bascou J, Wollman F-A, Nugent JHA, Purton S. (1995). Nuclear mutants of *Chlamydomonas reinhardtii* defective in the biogenesis of the cytochrome b6 fcomplex. *Plant Mol Biol.* **29**: 921 932.

Hansen MT. (1982). Rescue of mitomycin C- or psoralen-inactivated *Micrococcus radiodurans* by additional exposure to radiation or alkylating agents. *J Bacteriol*; **152:** 976-982.

Harris E. (1989). The Chlamydomonas Sourcebook. John Wiley, New York.

Havaux M, and Niyogi KK. (1999). The violaxanthin cycle protects plants from photooxidative damage by more than one mechanism. *Proceedings of the National Academy of Sciences of the United States of America References* 83 *USA*; **96**: 8762-8767.

Havaux M, Dall'Osto L, Cuiné S, Giuliano G, and Bassi R. (2004). The effect of zeaxanthin as the only xanthophyll on the structure and function of the photosynthetic apparatus in *Arabidopsis thaliana*. *J Biol Chem.*; **279(14)**: 13878-88.

Hellweg CE, and Baumstark-Khan C. (2007) Getting ready for the manned mission to Mars: the astronauts' risk from space radiation. *Naturwissenschaften*; **94(7)**: 517-26.

Herrin DL, Battey JF, Greer K, and Schmidt GW. (1992). Regulation of chlorophyll apoprotein expression and accumulation. Requirements for carotenoids and chlorophyll. *J Biol Chem.;* **267(12)**: 8260-9.

Hideg E, Vass I, Kalai T and Hideg K. (2000). Singlet oxygen and photo-oxidative stress *Methods Enzimol*; **319**: 77-85.

Hirschberg J. (1998). Molecular biology of carotenoid biosynthesis. Britton G, Liaaen-Jensen S, Pfander H, eds. 1998. *Carotenoids: Biosynthesis and Metabolism*. Basel: Birkhäuser, pp. 149–94.

Horneck G, Eschweiler U, Reitz G, Wehner J, Willimek R, and Strauch K. (1995). Biological responses to space: results of the experiment "Exobiological Unit" of ERA on EURECA. *Adv Space Res;* **16**: 105-18.

Johanningmeier U, and Heiss S. (1993). Construction of a *Chlamydomonas reinhardtii* mutant with an intronless *psbA* gene. *Plant Mol. Biol*., **22**: 91-99.

Jolivet E, Matsunaga F, Ishino Y, Forterre P, Prieur D, and Myllykallio H. (2003). Physiological responses of the hyperthermophilic Archaeon"*Pyrococcus abyssi*" to DNA damage caused by ionizing radiation. *J Bacteriol;* **185**: 3958-3961.

Karabin GD, Farley M, and Hallick RB. (1984). Chloroplast gene for M, 32,000 polypeptide of photosystem II in *Euglena gracilis* is interrupted by four introns with conserved boundary sequences. *Nucl. Acids. Res*., **12**: 5801-5812.

Kargul J and Barber JT. (2008). Photosynthetic acclimation: structural reorganisation of light harvesting antenna–role of redox-dependent phosphorylation of major and minor chlorophyll a/b binding proteins. *FEBS Journal*; **275: 1056–1068.**

Keller M, and Stutz E. (1984). Structure of the *Euglena gracilis* chloroplast gene (*psbA*) coding for the 32-kDa protein of Photosystem II. *FEBS Lett*.; **175**: 173-177.

Kim HS, Chung CH, Kang MS, and Ha DB. (1991). Okadaic acid blocks membrane fusion of chick embryonic myoblasts in culture. *Biochem. Biophys. Res. Commun*., **176:** 1044-1050.

Kordyum EL. (1997). Biology of plant cells in microgravity and under clinostating. *Int Rev Cytol*.;**171**: 1-78.

Kranz AR, Bork U, Bucker H, and Reitz G. (1990) Biological damage by ionizing cosmic rays in dry Arabidopsis seeds. *Int. J. Rad.Appl. Instrum D.;* **17**: 155-65.

Ledford HK, and Niyogi KK. (2005). Singlet oxygen and photo-oxydative stress management in plants and algae. *Plant Cell Environ*; **28**: 1037-1045.

Lefebvre PA and Silflow CD. (1999). *Chlamydomonas*: the cell and its genomes. *Genetics*; **151(1):** 9-14.

Linden H. (1999). Carotenoid hydroxylase from *Haematococcus pluvialis*: cDNA sequence, regulation and functional complementation. *Biochimica et Biophysica Acta;* **1446**: 203–12.

Lindgren LO, Stålberg KG, and Höglund AS. (2003). Seed-specific overexpression of an endogenous Arabidopsis phytoene synthase gene results in delayed germination and increased levels of carotenoids, chlorophyll, and abscisic acid. *Plant Physiol. Jun;* **132(2)**:779-85.

Livak KJ, and Schmittgen TD. (2001). Analysis of relative gene expression data using real-time quantitative PCR and the $2^{-\Delta\Delta CT}$ method. *Methods;* **25**: 402 – 408.

Lotan T and Hirschberg J. (1995). Cloning and expression in *Escherichia coli* of the gene encoding beta-C-4- oxygenase, that converts beta-carotene to the ketocarotenoid canthaxanthin in *Haematococcus pluvialis*. *FEMS Microbiology Letters;* **364**: 125–28.

Lydakis-Simantiris N, Ghanotakis DF, and Babcock GT. (1997). Kinetic isotope effects on the reduction of the YZ radical in oxygen-evolving and tris-washed Photosystem II membranes by time-resolved EPR. *Biochim Biophys Acta;* **1322**: 129–140.

Manuell AL, Beligni MV, Elder JH, Siefker DT, Tran M, Weber A, McDonald TL, Mayfield SP. (2007). Robust expression of a bioactive mammalian protein in *Chlamydomonas* chloroplast. *Plant Biotechnol J.;* **5(3):** 402-12.

Mattoo AK, Marder JB, and Edelman M. (1989). Dynamics of the photosystem II reaction center. *Cell;* **56:** 241–246.

Mayer MP, Beyer P, and Kleinig H. (1990). Quinone compounds are able to replace molecular oxygen as terminal electron acceptor in phytoene desaturation in chromoplasts of Narcissus pseudonarcissus *L. Eur J Biochem.*; **191(2)**: 359-63.

Mayfield SP, Manuell AL, Chen S, Wu J, Tran M, Siefker D, Muto M, Marin-Navarro J. (2007). *Chlamydomonas reinhardtii* chloroplasts as protein factories. *Current Opinion in Biotechnology*; **18(2)**: 126-33.

Melis A, Neidhardt J, Benemann JR. (1999). *Dunaliella salina* (Chlorophyta) with small chlorophyll antenna sizes exhibit higher photosynthetic productivities and photon use efficiencies than normally pigmented cells. *J Appl Phycol;* **10**: 515–525.

Mendez-Alvarez S, Leisinger U, and Eggen RI. (1999). Adaptive responses in *Chlamydomonas reinhardtii*. *Int Microbiol.*; **2(1)**: 15-22.

Merchant SS, Prochnik SE, Vallon O et al. (2007). The *Chlamydomonas* genome reveals the evolution of key animal and plant functions. *Science;* **12**; **318**: 245-50.

Mitchell P. (1961). Coupling of phosphorylation to electron and hydrogen transfer by a chemi-osmotic type of mechanism. *Nature;* **191**: 144–148.

Mozzo M, Dall'Osto L, Hienerwadel R, Bassi R, and Croce R. (2008). Photoprotection in the antenna complexes of photosystem II: role of individual xanthophylls in chlorophyll triplet quenching. *J Biol Chem.*; **283(10)**: 6184-92.

Mulo P, Sakurai I, and Aro EM. (2012). Strategies for *psbA* gene expression in cyanobacteria, green algae and higher plants: from transcription to PSII repair. *Biochim Biophys Acta.*; **1817(1)**: 247-57.

Nechitailo G, and Gordeev A. (2001). Effect of artificial electric fields on plants grown under microgravity condition. *Adv Space Res*; **28**: 629-631.

Nedukha EM. (1997). Effects of microgravity on the structure and function of plant cell walls. *Int Rev Cytol.*; **170**: 39-77.

Nedukha O, Brown CS, Kordyum E, and Piastuch WC. (1999). Electron-cytochemical study of Ca2+ in cotyledon cells of soybean seedlings grown in microgravity. *J Gravit Physiol.*; **6(1)**: 123-4.

Nishiyama Y, Allakhverdiev SI, and Murata N. (2006). A new paradigm for the action of reactive oxygen species in the photoinhibition of photosystem II. *Biochem Biophys Acta;* **1757**: 742-749.

Niyogi KK, Bjorkman O, and Grossman AR. (1997). Chlamydomonas Xanthophyll Cycle Mutants Identified by Video Imaging of Chlorophyll Fluorescence Quenching. *Plant Cell.*; **9(8)**:1369-1380.

Niyogi KK, Björkman O, and Grossman AR. (1997b). The roles of specific xanthophylls in photoprotection. *Proc. Natl. Acad. Sci. USA* **94;** 14162–14167.

Oettmeier W. (1992). Herbicides of photosystem II. In: J. Barber (Ed), The Photosystems: Structure, Function and Molecular Biology, Elsevier, Amsterdam, pp. 349-408.

Oettmeier W. (1999). Herbicide resistance and supersensitivity in photosystem II. *Cell Mol Life Sci.*; **55(10)**: 1255-77.

Ohad N, and Hirschberg J. (1992). Mutations in the D1 subunit of photosystem II distinguish between quinone and herbicide binding sites. *Plant Cell.*; **4(3)**: 273-82.

Palmer JD, Boyntonn EJ, Gillham W, and Harris H. (1985). Evolution and recombination of the large inverted repeat in Chlamydomonas chloroplast DNA, pp. 269-278 in The Molecular Biology of the Photosynthetic Apparatus, edited by K. E. STEINBACKS,. BONITZ, C. J. ARNTZEN aLn.d B OCORADC. Old Spring Harbor Laboratory,C old Spring Harbor, N.Y.

Polle JE, Niyogi KK, and Melis A. (2001). Absence of lutein, violaxanthin and neoxanthin affects the functional chlorophyll antenna size of photosystem-II but not that of photosystem-I in the green alga *Chlamydomonas reinhardtii*. *Plant Cell Physiol.*; **42(5)**: 482-91.

Popova AF, and Shniukova EI. (1995). Ultrastructure of chloroplasts and activity of amylases in Chlorella cells during space flight. *Tsitol Genet.*; **29(2)**: 41-5.

Preiss S, Schrader S and Johanningmeier U. (2001). Rapid, ATPdependent degradation of a truncated D1 protein in the chloroplast. *Eur J Biochem;* **268**: 4562–4569

Rea G, Lambreva M, Polticelli F, Bertalan I, Antonacci A, Pastorelli S, Damasso M, Johanningmeier U, Giardi MT. (2011). Directed evolution and in silico analysis of reaction centre proteins reveal molecular signatures of photosynthesis adaptation to radiation pressure. *PLoS One.*; **6(1)**: e16216

Rochaix JD. (1995). *Chlamydomonas reinhardtii* as the photosynthetic yeast. *Annual review of genetics*; **29**: 209-30.

Ruf S, Karcher D, and Bock R. (2007). Determining the transgene containment level provided by chloroplast transformation. *Proceedings of the National Academy of Sciences of the United States of America*; **104**: 6998-7002.

Saakov VS. (2003). Specific effects induced by gamma-radiation on the fine structure of the photosynthetic apparatus: evaluation of the pattern of changes in the high-order derivative spectra of a green leaf in vivo in the red spectral region. *Biochem Biophys;* **388:** 22-8.

Sakashita T, Doi M, Nakamura Y, Fuma S, Ishii N, Takeda H. (2002). Gamma-irradiation effect: variation of photosynthetic activity of Euglena. *Biomed Environ Sci;* **15**: 261-7.

Sandmann G. (2002). Molecular evolution of carotenoid biosynthesis from bacteria to plants. *Physiologia Plantarum;* **116**: 431–40.

Santosa S, and Jones PJ. (2005). Oxidative stress in ocular disease: does lutein play a protective role? *CMAJ.*; **173(8)**: 861-2.

Schledz M, Al-Babili S, von Lintig J, Haubruck H, Rabbani S, Kleinig H, and Beyer P. (1996). Phytoene synthase from *Narcissus pseudonarcissus*: functional expression, galactolipid requirement, topological distribution in chromoplasts and induction during flowering. *The Plant Journal;* **10**: 781– 92.

Schloss JA. (1990). A Chlamydomonas gene encodes a G protein beta subunit-like polypeptide. *Mol Gen Genet;* **221**:443–452.

Standfuss J, van Scheltinga ACT, Lamborghini M, and Ku¨hlbrandt W. (2005). Mechanisms of photoprotection and nonphotochemical quenching in pea light-harvesting complex at 2.5 A ° resolution. *EMBO J*; **24**: 919–928.

Steinbrenner J, and Linden H. (2001). Regulation of two carotenoid biosynthesis genes coding for phytoene synthase and carotenoid hydroxylase during stress-induced astaxanthin formation in the green alga *Haematococcus pluvialis*. *Plant Physiology;* **125**: 810–17.

Steinbrenner J, and Linden H. (2003). Light induction of carotenoid biosynthesis genes in the green alga *Haematococcus pluvialis*: regulation by photosynthetic redox control. *Plant Molecular Biology;* **52**: 343–56.

Strasser RJ, Srivastava A, and Govindjee. (1995). Polyphasic chlorophyll a fluorescence transient in plants and cyanobacteria. *Photochem Photobiol,* **61**: 32-42.

Sun Z, Gantt E, and Cunningham FX Jr. (1996). Cloning and functional analysis of the *β*-carotene hydroxylase of *Arabidopsis thaliana*. *The Journal of Biological Chemistry;* **271**: 24349– 53.

Svensmark H. (2000). Cosmic Rays And Earth's Climate. *Space Science Reviews;* **93:** 175–185.

Svensson B, Vass I, and Styring S. (1991). Sequence analysis of the Dl and D2 reaction center proteins of photosystem II. *Z. Naturforsch*., **46c**: 765-776.

Takahashi A, Ohnishi K, Takahashi S, Masukawa M, Sekikawa K, Amano T, Nakano T, Nagaoka S, and Ohnishi T. (2001). Differentiation of Dictyostelium discoideum vegetative cells into spores during Earth orbit inspace. *Adv Space Res.;* **28:** 549-53.

Tam L-W, and Lefebvre PA. (1993). Cloning of flagellar genes in *Chlamydomonas reinhardtii* by DNA insertional mutagenesis. *Genetics,* **135**: 375-384

Tellenbach M. (1984). Herbizidresistenz und Pigmentdefizienz, Ph.D. thesis, University of Bern, Switzerland.

Tsimilli-Michael M. and Strasser RJ. (2008). Experimental resolution and theoretical complexity determine the amount of information extracTable from the chlorophyll fluorescence transient OJIP. *Photosynthesis. Energy from the Sun*; **5:** 697–702.

Turmel M, Boulanger J, and Lemieux C. (1989). Two group-I introns with long internal open reading frames in the chloroplast *psbA* gene of *Chlamydomonas moewusii*. *Nucleic Acids Res,* **10**: 3875-3887.

Turner JE. (1995). Atoms, Radiation, and Radiation Protection, Wiley, New York, Chapter 5 “Interaction of heavy charged particles with matter”.

Van Oort B, van Hoek A, Ruban AV, van Amerongen H. (2007). Equilibrium between quenched and nonquenched conformations of the major plant light-harvesting complex studied with highpressure time-resolved fluorescence. *J Phys Chem B;* **111**: 7631–7637.

Venkateswaran A, Mcfarlan SC, Ghosal D, Minton KW, Vasilenko A, Makarova KA, Wackett P, and Daly MJ. (2000). Physiologic Determinants of Radiation Resistance in Deinococcus radiodurans. *Appl Environ Microbiol;* **66:** 2620-2626.

Vermaas WFJ, and Ikeuchi M. (1991). in The Photosynthetic Apparatus: Molecular Biology and Operation (Bogorad, L., & Vasil, I. K., Eds.) Vol. 7B, pp 25-1 11, Academic Press, San Diego.

Von Lintig J, Welsch R, Bonk M, Giuliano G, Batschauer A, and Kleinig H. (1997). Light-dependent regulation of carotenoid biosynthesis occurs at the level of phytoene synthase expression and is mediated by phytochrome in *Sinapis alba* and *Arabidopsis thaliana*. *The Plant Journal;* **12**: 625–34.

Vukich M, Ganga PL, Cavalieri D, Rizzetto L, Rivero D, Pollastri S, Mugnai S, Mancuso S, Pastorelli S, Lambreva M, Antonacci A, Margonelli A, Bertalan I, Johanningmeier U, Giardi MT, Rea G*;* Pugliese M, Roca V, Zanini A. (2011). BIOKIS: a model payload for multidisciplinary experiments in microgravità. *MicrigravSciTech;* (*Submittet*,).

Yashar M. Feyziyev. (2010). Oxygenic Photosynthesis: An Introduction#. Proceedings of ANAS (Biological Sciences); **65(5-6)**: 71-82.

Zeng XQ, Chow WS, Su LJ, Peng XX, and Peng CL. (2010). Protective effect of supplemental anthocyanins on Arabidopsis leaves under high light. *Physiol Plant;* **138**: 215–225.

Zhang JJ, Ying J, Chang SH, Li B, Li ZS. (2003). Cloning and expression analysis of violaxanthin deepoxidase (*vde*) cDNA in wheat. *Acta Botanica Sinica*; **45**: 981–85.

Zhang L, and Aro EM. (2002). Synthesis, membrane insertion and assembly of the chloroplast-encoded D1 protein into photosystem II. *FEBS Lett*.; **512(1-3)**: 13-8.